Naval Research Laboratory
Stennis Space Center, MS 39529-5004

NRL/MR/7432--93-7082

A Geoacoustic Model for Fine-Grained, Unconsolidated Calcareous Sediments (ARSRP Natural Laboratory)

FREDERICK A. BOWLES

Seafloor Sciences Branch
Marine Geosciences Division

March 9, 1994

REPORT DOCUMENTATION PAGE

Form Approved OBM No. 0704-0188

1. Agency Use Only *(Leave blank).*	2. Report Date.	3. Report Type and Dates Covered.
	March 9, 1994	Final

4. Title and Subtitle.

A Geoacoustic Model for Fine-Grained, Unconsolidated Calcareous Sediments (ARSRP Natural Laboratory)

5. Funding Numbers.

Program Element No.	0601153N
Project No.	03204
Task No.	040
Accession No.	DN250051
Work Unit No.	745153

6. Author(s).

Frederick A. Bowles

7. Performing Organization Name(s) and Address(es).

Naval Research Laboratory
Marine Geosciences Division
Stennis Space Center, MS 39529-5004

8. Performing Organization Report Number.

NRL/MR/7432--93-7082

9. Sponsoring/Monitoring Agency Name(s) and Address(es).

Office of Naval Research
800 N. Quincy Street
Arlington, VA 22217

10. Sponsoring/Monitoring Agency Report Number.

NRL/MR/7432--93-7082

11. Supplementary Notes.

12a. Distribution/Availability Statement.

Approved for public release; distribution is unlimited.

12b. Distribution Code.

13. Abstract *(Maximum 200 words).*

This report presents a geoacoustic model that is broadly applicable to deep ocean areas that are covered with soft, fine-grained, predominantly calcareous sediment. The model is based on a compilation and assessment of sediment (geoacoustic) properties deemed important as input parameters to acoustic field models. Physical properties measurements (compressional wave velocity, shear wave velocity, density, porosity) extracted from Deep Sea Drilling Project and Ocean Drilling Program Initial Reports provide the bulk of the accumulated data. Attenuation data and additional shear wave data were obtained from other sources. The data are presented as: (1) statistical summaries; (2) cross-plots illustrating the relationships between properties; and (3) regression equations. Empirically derived relationships commonly used to prepare geoacoustic models are not employed by this model. A discussion is presented in order to document the reasoning and, ultimately, the choices made in constructing the model.

14. Subject Terms.

Geoacoustics, Geologic Models, Seafloor, Sediments

15. Number of Pages. 55

16. Price Code.

17. Security Classification	18. Security Classification of Report.	19. Security Classification of This Page.	20. Limitation of Abstract. of Abstract.
Unclassified	Unclassified	Unclassified	SAR

A GEOACOUSTIC MODEL FOR FINE-GRAINED, UNCONSOLIDATED, CALCAREOUS SEDIMENTS (ARSRP NATURAL LABORATORY)

OBJECTIVE:

The long-range scientific goal of the Acoustic Reverberation Special Research Program (ARSRP) is to understand and predict ocean broadband reverberation at low frequencies (50-1000 Hz) over long propagation paths (up to 1000 km). To implement this goal, the concept of Natural Laboratories in the Atlantic and Pacific Oceans (Tucholke et al., 1991) was developed as an effective means for studying geological and geophysical variability of seabed properties that determine acoustic bottom/subbottom reverberation. This memorandum report, in support of ARSRP reverberation modeling in the Atlantic area, represents a compilation of sediment (geoacoustic) properties deemed important as input parameters to acoustic field models.

APPROACH:

Because the volume of published sediment geoacoustic data for the Atlantic Natural Laboratory region is small, the database was expanded to include geoacoustic data from other ocean basin areas in order to obtain better statistical representations for each parameter. The Natural Laboratory is located east of Bermuda on the flanks of the Mid-Atlantic Ridge and has bottom depths that are generally shoaler than the calcium compensation depth. It is assumed, therefore, that the sediments will be pelagic, dominantly fine-grained, calcareous, and will have generally the same physical characteristics as calcareous sediments in other open ocean areas (i.e., the deposition of a calcareous clay/ooze is essentially the same for all deep-ocean areas).

The geoacoustic data are derived primarily from extensive laboratory and shipboard measurements made on Deep Sea Drilling Project and Ocean Drilling Program (DSDP/ODP) cores and published in the DSDP/ODP cruise reports (Table 1). Compositionally, the sediments in the database range in carbonate content from 30% to nearly 100% (Fig. 1). Lithologically, they are primarily oozes and chalks. A substantial amount of geoacoustic data in the DSDP/ODP reports is not

Table 1. DSDP and ODP Sources of Sediment Data

DSDP Site	Leg	Samples	Location
400A	48	30	North Atlantic
401	"	22	" "
516F	72	18	South Atlantic
ODP Site	**Leg**	**Samples**	**Location**
628A	101	7	Bahama Bank
630	"	10	" "
632A	"	6	Exuma Sound
633	"	4	" "
647A	105	15	Labrador Sea
657A	108	41	Equatorial Atlantic
657B	"	5	" "
662A	"	12	" "
663A	"	8	" "
664B	"	12	" "
705A	115	6	Mascarene Plateau
706A	"	13	" "
706B	"	12	" "
707A	"	16	"
707B	"	14	" "
707C	"	6	" "
708A	"	28	" "
709A	"	43	" "
709B	"	31	" "
710A	"	2	" "
710B	"	2	" "
711A	"	11	" "
711B	"	3	" "
712A	"	9	" "
713A	"	1	" "
714A	"	41	" "
714B	"	18	" "
728A	117	10	Arabian Sea
730A	"	12	" "
731A	"	21	" "
744A	119	12	Kerguelen Plateau
758A	121	47	Ninetyeast Ridge
760A	122	16	Wombat Plateau
761B	"	35	" "
762B	"	24	Exmouth Plateau
762C	"	40	" "
763A	"	23	" "
764A	"	7	Wombat Plateau
764B	"	2	" "
765B	123	5	Argo Abyssal Plain
766A	"	8	Exmouth Plateau
768B	124	12	Sulu Sea
770B	"	4	Celebes Sea
787B	126	5	Izu-Bonin Basin
790C	"	5	Minami-Sumisu Basin
791B	"	16	" " "
793A	"	9	Izu-Bonin Basin
793B	"	11	" " "

included in the database for the following reasons: (1) geoacoustic measurements with no accompanying carbonate content information were excluded. The importance of clearly defining sediment type (i.e., ooze vs. clay) in relationship to the various properties is important for the extrapolation of these properties to unsampled or poorly sampled areas of the Natural Laboratory; and (2) graphical presentations of analytical results were usually not detailed enough to be usable.

Results from extensive studies on the acoustic and physical properties of deep-sea carbonate sediments reported by Johnson et al. (1977), Milholland et al. (1980), Mayer (1979), and Hamilton et al. (1982) are not included in this compilation but are summarized along with this study in Table 2. The study by Hamilton et al. (1982) consists of 323 samples and includes the work of Johnson et al. (1977) and Mayer (1979). The samples, which are from the Ontong-Java Plateau and the eastern equatorial Pacific, represent the upper 9 m of sediment; roughly half of the samples occur in the top 45 cm of sediment. Milholland (1978) made a systematic study of 269 DSDP core samples representing a complete ooze-chalk-limestone sequence (1262 m) on the Ontong-Java Plateau (sites 288 and 289).

Relative to the geoacoustic properties previously mentioned, compressional wave attenuation, shear wave attenuation, and shear wave velocity are sparsely represented in the literature. Consequently, in order to obtain reasonable estimates of these properties, all available data were used that related to fine-grained, or predominantly fine-grained, sediments. In cases where the sediment is designated as turbidite, sand-silt-clay, or mud, it is assumed that there is a substantial fine-grained component. In abyssal plain areas, for example, turbidite layers are usually thin relative to the clay-ooze intervals that separate them. In the case of shear wave attenuation, so little data are available that some measurements made in sandy sediments are included in the database.

The data in this report are presented as (1) tables that summarize various statistical parameters for the sediment geoacoustic properties previously mentioned, (2) cross plots that illustrate the relationships between various properties, and (3) a geoacoustic model based on 1 and 2. Curve fits to the data are provided by regression equations (data

Table 2. Average properties of calcareous sediments (standard deviations shown in brackets).

	ρ(g/cm^3)	n (%)	Vp (km/sec)	Vs (m/sec)	Lithology
This Study	1.67 (0.15)	63.9 (8.6)	1.57 (0.10)	94 (53.1)	ooze
	1.87 (0.01)	53.6 (8.2)	1.76 (0.17)	198 (53.5)	chalk
Hamilton et al. (1982)					
Ontong-Java Plateau	1.48 (0.03)	72.7 (1.73)	1.54 (8.2)	---------	ooze
East Pacific	1.38 (0.09)	78.6 (5.16)	1.53 (7.2)	---------	ooze
Milholland (1978)					
Sites 288/289	1.69 (0.10)	----------	1.72 (0.08)	---------	ooze
Sites 288/289	1.90 (0.10)	----------	2.21 (0.27)	910 (0.23)	chalk

*Both Hamilton and Milholland studied samples from the Ontong-Java Plateau. However, the Hamilton samples were all from box cores and are essentially surface and near-surface samples. Thus, the average values will not compare particularly well with this study or Milholland's, both of which take into account samples that are from greater depths (i.e., several hundred meters).

permitting). Regression analysis represents a means of quantifying the relationships among sediment properties. The equations can be used to predict values for a desired property when values of another physically related property are known.

When summarizing analytical measurements (mean values, regression equations, etc.) from a variety of sources (Table 1), errors are inherent due to differences in measurement technique, instrument calibration and precision, sample disturbance, sampling bias, etc. Nevertheless, Table 2 shows that the results of this study compare well with similar studies. The difficulty in measuring shear waves and determining attenuation in sediments, including the fact that the mechanisms governing these parameters are poorly understood, make them the least reliable of all the geoacoustic parameters.

DISCUSSION OF DATA:

General:

Measured geoacoustic values extracted from the DSDP/ODP literature are summarized in Table 3. The wide range in values is due largely to the factors mentioned above but also because the individual values represent a wide sampling range within the sediment column. Chalks and oozes are listed separately because they are (usually) lithologically distinct and, therefore, have different ranges of values for the same properties. DSDP lithologic nomenclature conventions (Winterer et al., 1973) define oozes as soft and readily deformed using the finger or broad spatula blade. Chalks, which are also soft, are less easily deformed (i.e., chalks are partly indurated oozes).

Figures 2, 3, and 4 show reasonably good empirical relationships between compressional wave velocity, bulk density, and porosity. Within the limits defined in Table 3, compressional velocity, shear velocity, and bulk density all increase in magnitude with depth below the seafloor, while porosity decreases (Figs. 5, 6, 7, and 8). Curve fits for these depth plots appeared reasonable only in the case of bulk density (Fig. 6) although a fit is provided for shear wave velocity as well (Fig. 8). No relationship was established between shear wave velocity and the other properties.

Table 3. Statistics of Sediment Properties Measurements From DSDP/OPD Samples (Table 1).

Sediment Property	Mean	Max.	Min.	Std. Dev.	Std. Error	Total Samples
OOZES						
Bulk Density(g/cm^3)	1.67	2.32	1.13	0.15	0.007	464
Porosity (%)	63.9	88.0	32.0	8.6	0.401	464
P-wave Velocity (km/sec)	1.57	2.28	1.46	0.10	0.005	435
S-wave Velocity (m/sec)	93.9	347	23	53.1	3.491	230
Calcium Carbonate (%)	79.8	97	31	14.6	0.658	496
CHALKS						
Bulk Density (g/cm^3)	1.87	2.32	1.37	0.14	0.008	281
Porosity (%)	53.6	73	32	8.2	0.500	272
P-wave Velocity (km/sec)	1.76	2.30	1.48	0.17	0.011	253
S-wave Velocity (m/sec)	198	298	117	53.5	14.29	14
Calcium Carbonate (%)	70.8	100	30	20.2	1.188	290

Compressional velocity (Fig. 9), density (Fig. 10), and porosity (Fig. 11) appear to be independent of carbonate content. Hamilton et al. (1982) have noted that as carbonate content exceeds 75% velocities may increase due to the presence of coarse sand-sized particles (e.g., foraminifera tests). This database consists of deep-water oozes (2000-4000 m) containing little or no coarse material. Consequently, no increase in velocity is observed at carbonate percentages above 75%.

Hamilton et al. (1982) also noted a correlation between bulk density and percent carbonate in sample suites where changes in carbonate content are balanced by changes in biogenic silica content. If, on the other hand, the changes in carbonate content are balanced by changes in pelagic clay content (similar grain density as calcium carbonate) no usable relationship exists. Samples containing biogenic silica were omitted from the database forming this report. Therefore, it follows that no correlation was observed between bulk density and percent carbonate.

Compressional Wave Velocity:

Urmos and Wilkens (1993) observed that the presence of chalks coincided with greater scatter in their data. Likewise, the scatter in Figures 2-8, which includes both ooze and chalk data, is attributed mainly to chalks as demonstrated when these lithologies are separated. In Figure 12, for example, most of the oozes cluster above 250 m, whereas the chalks (Fig. 13) are widely scattered throughout the sediment column.

The observation that the oozes occur predominantly within the top 250 m of sediment suggests that soft, pelagic, carbonate oozes transition to chalks at roughly this depth. Urmos and Wilkens (1993) place the ooze-chalk transition nearer to 300 m. These observations are consistent with Schlanger and Douglas (1974) who defined a shallow-burial realm where gravitational compaction is the dominant process and cementation is a subordinate. The fact that chalks are found scattered throughout the entire depth range in Figure 13 indicates that the ooze-chalk transition is not strictly time and depth-of-burial dependent. Cementation can be enhanced in the shallow-burial realm for a variety of reasons, resulting in the development of chalk above 250 m. Rapid and extensive diagenesis is characteristic of carbonate

sediments of the Bahama Banks area. Exuma sound samples from ODP Site 633 account for all but one of the chalks that occur above 50 m in Figure 13.

The scatter exhibited in Figure 13 is an indication of the variation in lithification and/or cementation associated with chalks which, in turn, may cause uncertainty in their identification. A number of the "oozes" in Figure 12, for example, plot well outside the general cluster of points. These outlying velocities are more appropriate for chalks. Similarly, some "chalks" (Fig. 13) have velocities that are indicative of oozes. A simple linear fit can be applied to the ooze data above 250 m (Fig. 14). The fit is slightly improved in Figure 15 by assuming that velocities of 1.60 km/sec or above are indicative of chalk and that anything less is an ooze. Thus, some of the data in Figure 14 are excluded from Figure 15 while some of the data in Figure 13 are included. In Figures 16 and 17 bulk density and porosity have been "filtered" in a similar manner.

The regression equations in Figures 15-17 are useful for modeling the upper 250-300 m of pelagic sediment if one assumes that there are few if any chalk layers within this interval. This assumption may not be unrealistic. Sonic velocity logs recorded under laboratory conditions (see various DSDP/ODP reports), in addition to laboratory measurements made on discrete samples, typically represent the upper few hundred meters of sediment as having relatively uniform compressional wave velocity profiles (i.e., no large velocity spikes).

Urmos and Wilkens (1993) have reported a discrepancy between sediment properties measurements made in the laboratory and in situ values. They attribute this to the hydraulic rebound of pore water when sediment is transferred from ambient conditions to laboratory conditions. It is apparent from their work that laboratory measurements do not preserve the nature of the velocity gradients found in undisturbed deposits. As a result, they have derived an empirical velocity correction factor (ΔVp) that can be applied to unconsolidated calcareous sediments with carbonate contents greater than 60%. A corrected velocity profile, obtained by using their technique, is shown in Figure 15.

Shear Wave Velocity:

Propagating and receiving shear waves in unconsolidated sediments is difficult, even under controlled conditions. For this reason and those given in the earlier discussion of approach, one could question the reliability of the shear wave velocity data extracted from the DSDP/ODP reports. Although the scatter in the data is substantial in Figure 8, a linear curve fit of the data is provided, and the equation shown is used to compute curve 6 in Figure 18. For comparison, eight other curves (some commonly referenced) are shown, and their associated equations are listed below. The equations are indexed according to the number given to each curve in Figure 18.

1. $Vs = 78.89d^{0.312}$
2. $Vs = 116 + 4.65d$ (where d = 0-36 m)
   $Vs = 237 + 1.28d$ (where d = 36-120 m)
   $Vs = 322 + 0.58d$ (where d = 120-650 m)
3. $Vs = 42.7064d^{0.3069}$
4. $Vs = 62.5223d^{0.3537}$
5. $Vs = 96.7977d^{0.29326}$
6. $Vs = 77.463 + 0.24079d$
7. $Vs = 33.48 + 1.44d + (-3.79 \times 10^{-3})d^2 + 6.67 \times 10^{-6}d^3$
   This equation, which will reproduce the curve shown in Figure 18, is based on the relationships of Bryan and Stoll (1988) that require void ratio as an input. In the case of curve 7, void ratios were estimated from porosity values given in the geoacoustic model section of this report.
8. $Vs = 75.4 + 1.51d + (-5.47 \times 10^{-3})d^2 + 8.35 \times 10^{-6}d^3$
9. $Vs = 23.0d^{0.3}$. The initial value of 23.0 m/sec is the average shear wave velocity for the fine-grained sediments found in Table 1 from Richardson et al. (1987). The power of 0.3 with depth (d) is from Richardson et al. (1991).

It is evident in Figure 8 that most of the shear wave velocities in the top 100 m of sediment fall within 25-125 m/sec and that over the full depth range (300 m) most values are less than 200 m/sec. These values are significantly lower than predicted by curves 1, 2, 4, and 5 in Figure 18, but are in the range predicted by the other curves. Curves 6 and 9, in particular, are comparable to laboratory measurements made on carbonate sediments by Schultheiss (1985) and Lavoie and Anderson (1991).

Most of the equations above predict higher surface shear wave velocities than are usually measured in muddy sediments. Direct probe measurements by Richardson et al. (1991), for example, recorded velocities of 20-25 m/sec at 10-30 cm and 40-50 m/sec at 2 m depth as well as gradients of 4-17 s^{1}. All the curves, with the exception of 6, also predict a generally rapid increase in shear wave velocity with depth for the upper 50 m of sediment followed by a more gradual increase. The laboratory measurements by Schultheiss (1985), and Lavoie and Anderson (1991) do not show any significant depth dependence (maximum sample depth = 270 m) and, in this respect, their data agree more closely with curve 6 in Figure 18. The absence of any significant gradient in their data indicates, once again, that velocity measurements made in the laboratory do not reflect in situ conditions (Urmos and Wilkens, 1993). Indeed, the large gradients that characterize curves 1, 2, 4, and 5 are consistent with in situ measurements made in non-carbonate muddy sediments (Fig. 19) which record significant velocity gradients in the upper 20 m of sediment. For comparison, curves 1 and 4 (Fig. 18) are also plotted in Figure 19.

Compressional Wave Attenuation:

The most comprehensive compilations of attenuation measurements in marine sediments have been assembled by Hamilton (1972, 1976a, and 1987) and Kibblewhite (1989). The acoustic community continues, for the most part, to use the work of Hamilton for estimating attenuation in marine sediments (Kibblewhite, 1989). Hamilton's view, most recently stated in 1987, is that attenuation (α) varies with the first power of frequency (f) and can be expressed as a function of frequency in kilohertz:

$$\alpha(\text{dB/m}) = kf^n$$

where k(dB/m/kHz) is a constant and n is assumed to be 1.0. Thus, compressional wave attenuation can be calculated for any particular frequency using the above equation.

The linear frequency dependence of attenuation has been questioned (Stoll, 1977, 1985, and 1989). Moreover, attenuation versus frequency relationships indicate basic differences between the response of fluid-saturated, coarse-and fine-grained sediments (Stoll, 1985). The sediments within the Natural Laboratory area are assumed to be predominantly fine-grained. Therefore, only attenuation data relating to fine-grained sediments were taken from the compilations of Hamilton (1972, 1976a, and 1987) and used to generate Figure 20. Kibblewhite's review (1989) did not produce any additional attenuation data relating to fine-grained sediments and a search of 1989 to recent literature produced only three relevant publications (Chotiros et al., 1989; Richardson et al., 1992; and Rogers et al., 1993). Thus, virtually all published compressional wave attenuation measurements (Table 4), relating to fine-grained sediments, appear in Figure 20.

Of particular interest in Figure 20 is the nature of the relationship between attenuation and frequency. A curve fit of the data shows that attenuation is dependent on frequency to the power of 1.1115. Over the frequency range shown the attenuation can be calculated using the following equation:

$$\alpha(\text{dB/m}) = 0.000025312\ f^{1.1115}$$

The stippled area in Figure 20 corresponds to the range of predicted attenuation values for "silts" calculated from the Biot model (Stoll, 1985 and 1989). It can be seen that the power curve fit is more linear in appearance than the "silt" envelope. Nevertheless, the above equation will produce values that are generally consistent with the predicted range of attenuation values up to frequencies of about 100 kHz.

Strickly speaking, the data in Figure 20 do not support the linear dependence of attenuation and frequency as advocated by Hamilton

Table 4. Compressional Wave Attenuation Data

Reference	Publication Year	Material/Area	Depth (m)	Frequency (Hz)	Attenuation (dB/m)	K (dB/m/kHz)
Shumway	1960	clayey silt (ave.12)	0	20500	1.09	0.053
Shumway	1960	clayey silt (ave.16)	0	22800	1.67	0.0732
Shumway	1960	clayey silt (ave.20)	0	30400	3.2	0.105
Wood & Weston	1964	mud	0	4000	0.279	0.0698
Wood & Weston	1964	mud	0	8000	0.476	0.0595
Wood & Weston	1964	mud	0	16000	0.951	0.0594
Wood & Weston	1964	mud	0	32000	1.8	0.0564
Wood & Weston	1964	mud	0	48000	3.02	0.0663
Bennett	1966	abyssal plains (ave)	0	12000	0.7	0.058
Ulonska	1968	clayey silt	0	250000	26.2	0.105
McLeroy & DeLoach	1968	silty clay,(site 6)	0	15000	1.08	0.072
McLeroy & DeLoach	1968	clay-silt,(site 9)	0	15000	1.12	0.075
McCann & McCann	1969	clay	0	368000	31.9	0.087
Berzon et al.	1969	clay	140	25	0.0035	0.139
Schirmer	1971	mud (clay-silt)	0	1200	0.29	0.242
Anderson & Blackman	1971	calcareous clay	250	200	0.0031	0.016
Anderson & Blackman	1971	calcareous clay	250	315	0.0126	0.04
Anderson & Blackman	1971	calcareous clay	250	250	0.0069	0.028
Neprochnov	1971	layer1, Bengal Bay	350	110	0.0165	0.15
Neprochnov	1971	layer1, Arabian Sea	400	110	0.0156	0.142
Neprochnov	1971	layer1, S.Indian Ocn	200	110	0.02	0.182
Neprochnov	1971	layer1, N.Indian Ocn	400	110	0.0182	0.166
Neprochnov	1971	layer1, Japan Sea	250	110	0.02	0.182
Neprochnov	1971	layer1, Black Sea	350	110	0.0165	0.15
Neprochnov	1971	Ob Trench	350	110	0.0174	0.158
Hamilton	1972	clayey silt	0	7000	1.2	0.171
Hamilton	1972	clayey silt	0	14000	2.4	0.171
Hamilton	1972	clayey silt	0	14000	2.3	0.164
Hamilton	1972	clayey silt	0	14000	1	0.071
Hamilton	1972	clayey silt	0	14000	0.6	0.043
Hamilton	1972	clayey silt	0	23200	2.8	0.121
Hamilton	1972	clayey silt	0	25000	4	0.16
Hamilton	1972	clayey silt	0	100000	18	0.18
Tyce	1976	carbonate	28	4000	0.12	0.03
Dicus	1976	turbidite	106	65	0.002	0.031
Helmberger et al.	1979	? (Bering Sea)	150	10	0.000295	0.0295
Ferla et al.	1980	mud	0	100	0.0041	0.041
Ferla et al.	1980	mud	1	250	0.017	0.068
Wrolstad	1980	turbidite	228	80	0.004	0.05
Chapman	1980	turbidite	200	160	0.002	0.013
Mitchell & Focke	1980	turbidite	0	213	0.0085	0.04
Mitchell & Focke	1980	turbidite	0	213	0.0055	0.026
Rubano	1980	clay/silt	0	20	0.0006	0.03
Rubano	1980	clay/silt	0	250	0.0094	0.038
Hooper et al.	1981	turbidite	0	163	0.0054	0.033
Frisk et al.	1981	silt/clay	80	220	0.0015	0.007
Tyce	1981	clayey silt?	14	4000	0.29	0.072
Tyce	1981	clayey silt?	16	4000	0.25	0.062
Tyce	1981	clayey silt?	18	4000	0.29	0.072
Tyce	1981	hemipelagic turbid.	27	4000	0.26	0.065
Tyce	1981	hemipelagic turbid.	21	4000	0.19	0.048
Tyce	1981	hemipelagic turbid.	25	4000	0.28	0.07
Tyce	1981	hemipelagic clay	14	4000	0.26	0.065
Tyce	1981	clayey silt?	15	4000	0.21	0.052
Dicus & Anderson	1982	turbidite	0	65	0.0026	0.04
Dicus & Anderson	1982	turbidite	0	65	0.0033	0.051
Dicus & Anderson	1982	calcareous clay	0	65	0.0176	0.271
Dicus & Anderson	1982	turbidite	0	65	0.0013	0.02
Tindle	1982	silt/clay	50	80	0.0045	0.056
Tindle	1982	silt/clay	50	140	0.0078	0.056
Stoll & Houtz	1983	sand/silt/clay	350	60	0.00756	0.126
Stoll & Houtz	1983	sand/silt/clay	350	10	0.00013	0.013
Stoll & Houtz	1983	sand/silt/clay	350	20	0.00113	0.056
Focke	1983	silt/clay	0	200	0.006	0.027
Jacobson et al	1984	turbidite	0	95	0.004	0.042
Barker & Helmberger	1986	? (Bering Sea)	150	32	0.0014	0.045
Barker & Helmberger	1986	? (Bering Sea)	150	18	0.0005	0.027
Frisk et al.	1986	silt/clay	26	220	0.0039	0.018
Frisk et al.	1986	silt/clay	19	220	0.007	0.032
Duckworth & Baggeroer	1986	turbidite	100	27.5	0.0019	0.069
Chotiros	1989	clay (ave.26)	30	400000	39.1	0.098
Richardson et al.	1992	Holocenic clays	0	400000	59	0.15
Richardson et al.	1992	Hemipelgic silty clays	0	400000	50	0.12
Rogers et al.	1993	sand & silty clay	100	50	0.000557	0.0111
Rogers et al.	1993	sand & silty clay	100	75	0.000753	0.01
Rogers et al.	1993	sand & silty clay	100	175	0.00213	0.0123
Rogers et al.	1993	sand & silty clay	100	275	0.00361	0.0131
Rogers et al.	1993	sand & silty clay	100	375	0.00524	0.014
Rogers et al.	1993	sand & silty clay	100	525	0.00802	0.0153
Rogers et al.	1993	sand & silty clay	100	600	0.00955	0.0159

(1987), even for fine-grained sediments. Nevertheless, the relationship is close enough to being linear that a first order approximation of attenuation may be acceptable for purposes of acoustic modeling. A linear fit to the data produces that following equation:

$$\alpha(\text{dB/m}) = -0.027116 + 0.00010532x$$

For most of the frequency range shown in Figure 20 this equation provides attenuation values that are very close to the values derived from the power law equation, but it's use is not recommended. At 500 Hz both equations give essentially the same attenuation value (i.e., the curves intersect). Below 500 Hz, however, the values derived from the linear equation decrease rapidly (i.e., the linear curve drops rapidly away from the power curve); below 260 Hz they become negative. At frequencies above 100 kHz the power equation gives attenuation values that increase at a much faster rate than values derived from the linear equation (i.e., the curves diverge rapidly).

In Figure 21 the same attenuation data used for Figure 20 are expressed as the attenuation coefficient k and plotted against depth. Superimposed on the data are attenuation-depth profiles from Hamilton (1976a), Mitchell and Focke (1980), Jacobson et al. (1981), and Brienzo (1992). For the present, these profiles appear to be the only choices that modelers have for predicting compressional wave attenuation at significant depths in the sediment column. Although Hamilton's profile is widely used, it can seen that his silt-clay profile is based on sparse, scattered data (Fig. 22). When plotted with additional data, as in Figure 21, the curve fit is not improved. Jacobson's profile is based on attenuation values for a region of thick, sand/silt turbidite deposits (i.e., Bengal deep-sea fan) and, as such, may not be suitable for modeling most deep, open-ocean areas. Brienzo's profile is also from an area of turbidite deposition (Monterey Fan), yet the attenuation values are significantly lower than Jacobson's. Indeed, they are very close to values represented by the Mitchell-Focke profile that was derived from bottom loss data taken in a region of calcareous ooze/calcareous clay sediment. Considering sediment type, the Mitchell-Focke profile

represents a more appropriate choice for geoacoustic modeling in deep ocean areas. The following regression equation,

$$K = 0.0262 + 8.301\times10^{-5}d + (-2.483\times10^{-7})d^2 + 1.455\times10^{-7}d^3$$

where d = depth and K is in dB/m/kHz, will essentially reproduce their profile (for the upper 500 m of sediment). Matthews (1982) notes that the Mitchell-Focke attenuation values yield plane wave bottom loss calculations in close agreement with measured bottom loss values.

Shear Wave Attenuation:

Very little information is available regarding the variations of shear wave attenuation with depth, particularly in unlithified, high-porosity, fine-grained sediments (Table 5). For modeling purposes Hamilton (1976c, 1987) has assumed that shear wave attenuation varies with depth in the sea floor proportionally with compressional wave attenuation according to the following equation:

$$K_{Sz} = (K_{So}/k_{po})\, K_{pz}$$

Accordingly, shear wave attenuation can be expected to track the curves shown in Figure 21 but at much higher K values (Hamilton suggests a surface value of K = 17.3 for unconsolidated clays). This assumption, however, does not hold with more recent data.

Sauter (1987) used spectral ratios of Scholte waves to estimate 1/Q in the sediments for a deep-water site off the California coast. His work represents a well-constrained study detailing changes in shear wave attenuation within the upper 60 m of sediment. In Figure 23 Sauter's values for 1/Q have been converted to K(dB/m/kHz) and plotted with depth along with various shear wave attenuations reported by other investigators. Sauter's study indicates a much higher shear wave attenuation at the sediment surface (k = 40) than Hamilton (1976c) suggests, and also shows that the attenuation decreases rapidly within the upper 5 m of sediment. Between 5-20 m the change is more gradual, and from 20-60 m the attenuation is practically constant. Shear wave estimates reported by Jensen and Schmidt (1986), Carter et al. (1986), and Bromirski et al. (1992) for depths of 60 and 180 m

Table 5. Shear Wave Attenuation Data

Reference	Publication Year	Material/Area	Depth (m)	Frequency (Hz)	Attenuation (dB/m)	K (dB/m/kHz)
Bucker et al.	1964	sand	0	20	0.328	16.4
Bucker et al.	1964	sand	0	25	0.197	7.88
Warrick	1974	soft mud	5	5	0.095	18.9
Joyner et al.	1976	soft mud	0	5	0.284	56.8
Schirmer	1980	North Sea (130m)	15	4.5	0.007	1.56
Holt, et al.	1983	sand	2	35	0.6	17.1
Brocher et al.	1983	sand	7	5	0.0038	0.769
Jensen & Schmidt	1986	sand/silt	0	3	0.016	5.29
Jensen & Schmidt	1986	sand/silt	60	3	0.002	0.5
Rauch	1986	soft sediment (mud?)	15	3.5	0.0056	1.6
Carter et al.	1986	biosiliceous clay	180	18	0.0205	1.137
Sauter	1987	clay/ooze	12	4	0.01	2.43
Sauter	1987	clay/ooze	14	4	0.0085	2.13
Sauter	1987	clay/ooze	10	4	0.011	2.73
Sauter	1987	clay/ooze	6	4	0.02	5.05
Sauter	1987	clay/ooze	8	4	0.014	3.59
Sauter	1987	clay/ooze	40	4	0.0033	0.82
Sauter	1987	clay/ooze	60	4	0.0023	0.57
Sauter	1987	clay/ooze	20	4	0.0064	1.61
Sauter	1987	clay/ooze	16	4	0.0076	1.9
Sauter	1987	clay/ooze	18	4	0.0071	1.76
Sauter	1987	clay/ooze	1	4	0.112	28.06
Sauter	1987	clay/ooze	0.5	4	0.136	34.11
Sauter	1987	clay/ooze	0	4	0.164	40.97
Sauter	1987	clay/ooze	2	4	0.091	22.76
Sauter	1987	clay/ooze	3.5	4	0.039	9.74
Sauter	1987	clay/ooze	3	4	0.055	13.84
Sauter	1987	clay/ooze	2.5	4	0.072	17.95
Sereno	1990	zeolitic Clay	35	15	0.118	7.84
Muir et al.	1991	mud	2.5	4	0.017	4.22
Muir et al.	1991	mud	7.5	4	0.008	2.08
Muir et al.	1991	mud	5	4	0.012	3.01
Muir et al.	1991	mud	30	4	0.0047	1.17
Muir et al.	1991	mud	15	4	0.0054	1.34
Muir et al.	1991	mud	0	4	0.0345	8.64
Bromirski et al.	1992	biosiliceous clay	180	18	0.0025	1.4
Bromirski et al.	1992	biosiliceous Clay	180	3	0.0042	1.4

(Table 5), coincide with Sauter's profile and support the observation that attenuation is essentially constant below 20 m.

Decreasing shear wave attenuation in the upper 4 m of muddy sediment (Fig. 24) is also documented by Muir et al. (1991) from measurements made in short (6 m) boreholes. Interestingly, their results indicate that attenuation varies with frequency to the power of 1.5, contradicting Hamilton's (1987) recommendation that shear wave attenuation be considered to vary linearly with frequency. It is apparent in Figure 24 that the attenuation curves for the different frequencies converge in the upper 4 m of sediment. Figure 25 combines the data in Figure 24 with the data in Figure 23 for the upper 20 m of sediment and shows that shear attenuation at low frequencies (100 Hz and less) is most variable in the first 4-5 m of sediment and is essentially constant below about 12 m. A comparison (Fig. 26) of Sauter's data (1987) with Scholte wave data presented by Muir et al. (1991) also shows large differences in attenuation in the upper 5 m of sediment (due principally to different sediment types - see Table 5) and convergence of the data below about 20 m.

RESULTS:

The geoacoustic parameters (porosity, wet bulk density, compressional wave velocity and attenuation, shear wave velocity and attenuation) discussed in the previous section are presented below in the form of a geoacoustic model that incorporates the variations of each parameter to a depth of 300 m (estimated sediment thickness for a large, midocean ridge flank sediment pond).

GEOACOUSTIC MODEL:

Material Type	Depth (mbsf)	Vp (m/sec)	Vs (m/sec)	ρ (g/cm^3)	n (%)	Kp (dB/m-kHz)	Ks
Nannofossil	0	1487	23	1.574	68.1	0.0266	41.0
clay/ooze	1	1488	67	1.575	68.1	0.0267	28.1
	2	1490	80	1.576	68.0	0.0267	22.8
	5	1494	110	1.579	67.9	0.0268	6.93
	10	1502	145	1.583	67.7	0.0270	2.73
	20	1516	180	1.592	67.3	0.0275	1.61
	30	1531	208	1.600	66.9	0.0278	1.21
	40	1545	230	1.610	66.4	0.0282	0.82
	50	1559	249	1.618	66.0	0.0285	0.69
	60	1572	266	1.627	65.6	0.0292	0.57
	80	1599	294	1.644	64.8	0.0301	0.57
	100	1624	319	1.662	63.9	0.0310	0.57
	120	1649	340	1.679	63.1	0.0315	0.57
	140	1672	359	1.697	62.2	0.0322	0.57
	160	1695	376	1.714	61.4	0.0327	0.57
	180	1717	392	1.732	60.6	0.0331	0.57
	200	1738	407	1.749	59.8	0.0335	0.57
	220	1759	421	1.767	58.9	0.0337	0.57
	240	1778	434	1.784	58.1	0.0340	0.57
	260	1797	447	1.802	57.2	0.0342	0.57
	280	1816	459	1.819	56.4	0.0342	0.57
	300	1833	470	1.837	55.6	0.0338	0.57
Basalt		4100	2100	2.810		0.0200	0.07

Notes:

1. Depth:

   mbsf = meters below seafloor

2. Vp (Compressional wave velocity):

Vp = compressional wave velocity = 1.487 + 0.00013369d + ΔVp where d = depth(m) and $\Delta Vp = 0.66\ (1-e^{-0.00208d})$.

The first part of the above equation is the same as the equation shown in Figure 15 except that the initial velocity at d = 0 m has been changed from 1.529 km/sec to 1.487 km/sec. In situ measurements, even in clayey silts, record surficial velocities below 1500 m/sec (Hamilton, 1972). The initial velocity of 1.487 km/sec is taken from an equation derived by Lovell and Ogden (1984) for surficial carbonate samples.

ΔVp is a correction factor derived by Urmos and Wilkens (1993) to compensate for differences in log (in situ) and laboratory velocities measured in calcareous sediments having carbonate contents of 60% or greater. The majority of the samples compiled for this report have carbonate contents greater than 60% (see Figure 1 and Table 3).

3. Vs (Shear wave Velocity):

Vs = shear wave velocity = $62.5^{d0.3537}$ (from Lovell and Ogden, 1984)

Vs = 23.0 m/sec at d = 0 m is an average value derived from measurements reported by Richardson (1987; Table 1) for fine-grained (noncalcareous) sediments. Vs = 67 m/sec at d = 1 m is taken from the (overlapping) Muir, Stoll, Lewis, and Davis curves in Figure 19. Because these four curves coincide closely with curve 4 in Figure 18 (See Fig. 19), the equation representing curve 4 (above) is used to compute Vs for 2-300 m.

4. ρ (Bulk Density):

ρ = 1.5743 + 0.0008742d, where d = depth(m). This equation is derived from a linear curve fit of the data in Figure 16.

5. n (Porosity):

   $n = 143.46 + (-47.851\rho)$, where ρ = bulk density. This equation is derived from a linear curve fit of the data in Figure 4. The equation shown in Figure 17 will produce comparable values.

6. Kp (compressional wave attenuation):

   $Kp = 0.0266 + 6.9 \times 10^{-5}d + (-1.5 \times 10^{-7})d^2$, where d = depth(m)

   The above equation represents the Mitchell and Focke curve shown in Figure 21. The equation does not hold below 500 m.

7. Ks (shear wave attenuation):

   Ks values are picked directly from the attenuation model generated by Sauter (1987) and shown in Figures 26 and 27. Sauter's model is derived from measurements made at a deep water site (3800 m) near DSDP Site 469. Although the upper 42 m of sediment in this area is described as a clay with a carbonate content less than 30% (Yeats, et al., 1981), it is thought to be the best choice, at this time, for estimating attenuation as a function of depth in soft sediments regardless of carbonate content.

MODEL APPLICABILITY:

The model presented in this report is generic and should be applicable to most areas that are covered with soft, fine-grained, calcareous sediment. It is important to note, however, that high-resolution, deep-towed multichannel seismic data (Gettrust et al., 1988; Rowe and Gettrust, 1989; Rowe and Gettrust, 1992; Rowe and Gettrust, 1993) resolve significant lateral and vertical variability in compressional velocity over distances of about ten to one hundred meters. Fine-scale spatial variability such as this is not addressed by presently accepted geoacoustic modeling methods (Hamilton, 1972, 1976a, 1976b, 1987; Hamilton and Bachman 1982) nor by the model presented here. Moreover, these data reveal that compressional velocity gradients in the upper few hundred meters of the sediment column can be substantially lower than conventional geoacoustic models predict.

ACKNOWLEDGMENTS:

This work was supported by the Office of Naval Research-sponsored Acoustic Reverberation Special Research Program, Program Element 0601153N32, Project Number R0320404, Program Manager, Dr. Mohsen Badiey.

REFERENCES:

Anderson, R. S. and Blackman, A., 1971. Attenuation of low-frequency sound waves in sediments. J. Acoust. Soc. Am., 49(3), 786-791.

Barker, J. S. and Helmberger, D. V., 1986. A broad-band study of attenuation in ocean bottom sediments. In T. Akal and J. M. Berkson (eds)., Ocean Seismo-Acoustics, Plenum Press, New York, 609-621.

Bennett, Jr., L. C., 1966. In situ measurements of acoustic absorption in unconsolidated marine sediments. Ph.D. dissertation, Bryn Mawr College.

Berzon, I. S., Batnikova, L. I., and Mitronova, V. A., 1969. Shearwaves reflected from a thin high-speed layer. In I. S. Berzon (ed.), Shear Wave Propagation in Real Media, Consultants Bureau, New York, 154-162.

Brienzo, R. K., 1992. Velocity and attenuation profiles in the Monterey Deep-Sea Fan. J. Acoust. Soc. Am., 92(4), 21092125.

Brocher, T. M., Iwatake, B. T., and Lindwall, D. A., 1983. Experimental studies of low-frequency waterborne and sedimentborne acoustic wave propagation on a continental shelf. J. Acoust. Soc. Am., 74(3), 960-972.

Bromirski, P. D., Frazer, L. N., and Duennebier, F. K., 1992. Sediment shear Q_β from airgun OBS data. J. Int. Geophys., 465-485.

Bryan G. M. and Stoll R. D., 1988. The dynamic shear modulus of marine sediments. J. Acoust. Soc. Am., 83(6), 2159-2164.

Bucker, H. P., Whitney, J. A., and Keir, D. L., 1964. Use of Stoneley waves to determine the shear velocity in ocean sediments. J. Acoust. Soc. Am., 36(8), 1595-1596.

Carter, J. A., Sutton, G. H., and Suteau-Henson, A., 1986. Analysis of ocean-subbottom seismograph (OSS) data. In T. Akal and J. M.Berkson (eds.), Ocean Seismo-Acoustics, Plenum Press, New York, 553-563.

Chapman, N. R., 1980. Low frequency bottom reflectivity measurements in the Tufts Abyssal Plain. In W. A. Kuperman and F. B. Jensen (eds.), Bottom-Interacting Ocean Acoustics, Plenum Press, New York, 193-207.

Chotiros, N. P., 1989. High frequency acoustic penetration analysis. Applied Res. Labs., Univ. of Texas, Austin, ARL-TR-89-28.

Davies, D., 1965. Dispersed Stoneley waves on the ocean bottom. Bull. Seis. Soc. Am., 55(5), 903-918.

Dicus, R. L., 1976. Preliminary investigations of the ocean bottom impulse response at low frequencies. Naval Oceanographic Office Tech. Note 6130-4-76.

Duckworth, G. L. and Baggeroer, A. B., 1986. Estimation of ice surface scattering and acoustic attenuation in Arctic sediments from long-range propagation data. In T. Akal and J. M. Berkson (eds.), Ocean Seismo-Acoustics, Plenum Press, New York, 373-386.

Dicus, R. L. and Anderson, R. S., 1982. Effective low-frequency geo-acoustic properties inferred from measurements in the northeast Atlantic. Naval Research Laboratory, Stennis Space Center, MS, NORDA Report 21.

Ferla, M. C., Dreini, F. B., Jensen, F. B., and Kuperman, W. A., 1980. Broadband model/data comparisons for acoustic propagation in coastal waters. In W. A. Kuperman and F. B. Jensen (eds.), Bottom-Interacting Ocean Acoustics, Plenum Press, New York, 577-592.

Focke, K. C., 1983. Acoustic attenuation in ocean sediments found in shallow water regions. Masters Thesis, Univ. of Texas, Austin; also Applied Res. Labs., ARL-TR-84-6.

Frisk, G. V., Doutt, J. A., and Hays, E. E., 1981. Bottom interaction of low-frequency acoustic signals at small grazing angles in the deep ocean. J. Acoust. Soc. Am., 69(1), 84-94.

Frisk, G. V., Doutt, J. A., and Hays, E. E., 1986. Geoacoustic models for the Icelandic Basin. J. Acoust. Soc. Am., 80(2), 591-600.

Gabriels, P., Snieder, R., and Nolet, G., 1987. In situ measurements of shear-wave velocity in sediments with higher-mode Rayleigh waves. Geophys. Prospect., 35, 187-196.

Gettrust, J. F., Grimm, M., Madosik, S., and Rowe, M., 1988. Results of a deep-tow multichannel survey on the Bermuda Rise. Geophys. Res. Lett., 15, 1413-1416.

Hamilton, E. L., 1972. Compressional-wave attenuation in marine sediments. Geophys., 37(4), 620646.

Hamilton, E. L., 1976a. Sound attenuation as a function of depth in the deep sea floor. J. Acoust. Soc. Am., 59(3), 528-535.

Hamilton, E. L., 1976b. Shear wave velocity versus depth in marine sediments: a review. Geophysics, 41, 985-996.

Hamilton, E. L., 1976c. Attenuation of shear waves in marine sediments. J. Acoust. Soc. Am., 60(2), 334-338.

Hamilton, E. L., Berger, W. H., Johnson, T. C., and Mayer, L. A., 1982. Acoustic and related properties of calcareous deep-sea sediments. J. Sed. Petrology, 52, 733-753.

Hamilton, E. L. and Bachman, R. T., 1982. Sound velocity and related properties of marine sediments. J. Acoust. Soc. Am., 72(6), 1891-1904.

Hamilton, E. L., 1987. Acoustic properties of sediments. In A. Lara-Saenz, C. Ranz-Guerra, and C. Caro-Fite (eds.), Acoustics and Ocean bottom. Sociedad Espanola de Acustica, Instituto de Acustica-CSIC, F.A.S.E. Specialized Conference, Madrid, 3-58.

Helmberger, D. V., Engen, G., and Scott, P., 1979. A note on velocity, density, and attenuation models for marine sediments determined from multibounce phases. J. Geophs. Res., 84, 667-671.

Holt, R. M., Hovem, J. M., and Syrstad, J., 1983. Shear modulus profiling of near bottom sediments using boundary waves. In N. G. Pace (ed.), Acoustics and the Sea-Bed, Bath Univ. Press, Bath, UK, 317-325.

Hooper, M. S., Ingram, G. D., and Mitchell, S. K., 1981. Measurements and analysis of acoustic bottom interaction in the northwestern Mexican basin. Applied Res. Labs., Univ. of Texas, Austin, ARL-TR-81-37.

Jacobson, R. S., Shor, Jr., G. G., and Dorman, L.M., 1981. Linear inversion of body wave data-Part II: Attenuation versus depth using spectral ratios. Geophysics, 46(2), 152-162.

Jacobson, R. S., Shor, Jr., G. G., and Bee, M., 1984. A comparison of velocity and attenuation between the Nicobar and Bengal Deep Sea Fans. J. Geophys. Res., 89, 6181-6196.

Jensen, F. B. and Schmidt, H., 1986. Shear properties of ocean sediments determined from numerical modelling of Scholte wave data. In T. Akal and J. M. Berkson (eds.), Ocean Seismo-Acoustics, Plenum Press, New York, 683-692.

Johnson, T. C., Hamilton, E. L., and Berger, W. H., 1977. Physical properties of calcareous ooze: control by dissolution at depth. Mar. Geol. 24, 259-277.

Joyner, W. B., Warrick, R. E., and Oliver, III, A. A., 1976. Analysis of seismograms from a downhole array in sediments near San Francisco Bay. Bull. Seis. Soc. Am., 66(3), 937-958.

Kibblewhite, A. C., 1989. Attenuation of sound in marine sediments: a review with emphasis on new low frequency data. J. Acoust. Soc. Am., 86(2), 716-738.

Lavoie, D. and Anderson, A. 1991. Laboratory measurements of acoustic properties of periplatform carbonate sediments. In J. M. Hovem, M. D. Richardson, and R. D. Stoll (eds.), Shear Waves in Marine Sediments, Kluwer Academic Publishers, Dordrecht, The Netherlands, 111-120.

Lewis, B. T. R., 1991. Changes in P and S velocities caused by subduction related sediment accretion off Washington/Oregon. In J. M. Hovem, M. D. Richardson, and R. D. Stoll (eds.), Shear Waves in Marine Sediments, Kluwer Academic Publishers, Dordrecht, The Netherlands, 379-386.

Lovell, M. A. and Ogden, P., 1984. Remote assessment of permeability/thermal diffusivity of consolidated clay sediments. Final Report (EUR 9206 en) to Commission of the European Communities, Nuclear Science and Technology, Luxembourg, 168p.

Matthews, J. E., 1982. Geoacoustic models for the Straits of Sicily and Sardinia-Tunisia. Naval Research Laboratory, Stennis Space Center, MS, NORDA Technical Note 98.

Mayer, L. A.,1979. Deep sea carbonates: acoustic, physical, and stratigraphic properties. J. sed. Petrology, 49, 819-836.

McCann, C. and McCann, D. M., 1969. The attenuation of compressional waves in marine sediments. Geophysics, 34(6), 882-892.

McLeroy, E. G. and DeLoach, A., 1968. Sound speed and attenuation, from 15 to 1500 kHz, measured in natural sea-floor sediments. J. Acoust. Soc. Am., 44(4), 1148-1150.

Millholland, P., 1978. Geoacoustic model of deep sea carbonate sediments. Masters Thesis, Univ. of Hawaii, Honolulu.

Millholland, P., Manghnani, M. H., Schlanger, S. O., and Sutton, G. H., 1980. Geoacoustic modeling of deep-sea carbonate sediments. J. Acoust. Soc. Am., 68(5), 1351-1360.

Mitchell, S. K. and Focke, K. C., 1980. New measurements of compressional wave attenuation in deep ocean sediments. J. Acoust. Soc. Am., 67(5), 1582-1589.

Muir, T. G., Akal, T., Richardson, M. D., Stoll, R. D., Caiti, A., and Hovem,J. M., 1991. Comparison of techniques for shear wave velocityand attenuation measurements. In J. M. Hovem, M. D. Richardson, and R. D. Stoll (eds.), Shear Waves in Marine Sediments, Kluwer Academic Publishers, Dordrecht, The Netherlands, 283-294.

Neprochnov, Yu. P., 1971. Seismic studies of the crustal structure beneath the seas and oceans. Oceanology, 11, 709-715.

Ohta, Y. and Goto, N., 1978. Empirical shear wave velocity equations in terms of characteristic soil indexes. Earthquake Engineering and Structural Dynamics 6, 167.

Rauch, D., 1986. On the role of bottom interface waves in ocean seismo-acoustics: a review. In T. Akal and J. M. Berkson (eds.), Ocean Seismo-Acoustics, Plenum Press, New York, 623-641.

Richardson, M. D. Curzi, P. V., Muzi, E., Miaschi, B., and Barbagelata, A., 1987. Measurements of shear wave velocity in marine sediments. In A. Lara-Saenz, C. Ranz-Guerra, and C. Caro-Fite (eds.), Acoustics and Ocean bottom. Sociedad Espanola de Acustica, Instituto de Acustica-CSIC, F.A.S.E. Specialized Conference, Madrid, 75-84.

Richardson, M. D., Muzi, E., Miaschi, B., and Turgutcan F., 1991. Shear wave velocity gradients in near-surface marine sediment. In J. M. Hovem, M. D. Richardson, and R. D. Stoll (eds.), Shear Waves in Marine Sediments, Kluwer Academic Publishers, Dordrecht, The Netherlands, 295-304.

Richardson, M. D., Curzi, P. V., Muzi, E., Turgutcan, F., and Akal T., 1992. A generic geoacoustic model for the central Adriatic Sea. SACLANT Undersea Research Centre, SACLANTCEN REPORT SR-199, 89p.

Rogers, A. K., Yamamoto, T., and Carey, W., 1993. Experimental investigation of sediment effect on acoustic wave propagation in the shallow ocean. J. Acoust. Soc. Am., 93(4), 1747-1761.

Rowe, M. M. and Gettrust, J. F., 1989. DTAGS deep-towed seismic survey of the Blake-Bahama Basin NORDA Cruise 707A October-November 1988. Naval Research Laboratory, Stennis Space Center, MS, NORDA Technical Note 449.

Rowe, M. M. and Gettrust, J. F., 1992. Deep-Tow Acoustics/Geophysics System compressional velocity database. Naval Research Laboratory, Stennis Space Center, MS, NOARL Technical Note 257.

Rowe, M. M. and Gettrust, J. F., 1993. Fine structure of methane hydrate-bearing sediments on the Blake Outer Ridge as determined from deep-tow multichannel seismic data. J. Geophys. Res., 98(B1), 463-473.

Rubano, L. A., 1980. Acoustic propagation in shallow water over a low-velocity bottom. J. Acoust. Soc. Am., 67(5), 1608-1613.

Sauter, A. W., 1987. Studies of the upper oceanic floor using ocean bottom seismometers. Ph.D. Dissertation, Univ. of California, San Diego, 100p.

Schirmer, F., 1971. Eine untersuchung akustischer eigerschaften von sedimenten der Nord-and Ostsee. Ph.D. dissertation, Univ. of Hamburg.

Schirmer, F., 1980. Experimental determination of properties of the Scholte wave in the bottom of the North Sea. In W. A. Kuperman and F. B. Jensen (eds.), Bottom Interacting Ocean Acoustics, Plenum Press, New York, 285-298.

Schlanger, S. O. and Douglas, R. G., 1974. The pelagic ooze-chalk-limestone transition and its implications for marine stratigraphy. From Pelagic Sediments: On Land and Under the Sea. Internat. Assoc. Sediment-ologists Spec. Publ. No 1, K. J. Hsu and H. C. Jenkyns, eds., 447 p.

Schultheiss, P. J., 1985. Physical and geotechnical properties of sediments from the northwest Pacific: Deep Sea Drilling Project Leg 86. In G. R. Heath, L. H. Burckle, et al., Initial Reports of the Deep-Sea Drilling Project, 86. U.S. Government Printing Office, Washington, D.C., 701-722.

Sereno, Jr., T. J., 1990. Numerical modeling of water waves recorded by a subbottom seismometer in the southwest Pacific. J. Geophys. Res. 95, 2575-2591.

Shumway, G., 1960. Sound speed and absorption studies of marine sediments by a resonance method. Part I. Geophysics, 25(2), 451-467.

Stoll, R. D., 1977. Acoustic waves in ocean sediments. Geophysics, 42(4), 715-725.

Stoll, R. D. and Houtz, R. E., 1983. Attenuation measurements with sonobuoys. J. Acoust. Soc. Am., 73(1), 163-172.

Stoll, R. D., 1985. Marine sediment acoustics. J. Acoust. Soc. Am. 77(5), 1789-1799.

Stoll, R. D., 1989. Sediment Acoustics. Springer-Verlag, Berlin, Heidelberg, New York, 153 p.

Stoll, R. D., 1991. Shear waves in marine sediments - bridging the gap from theory to field applications. In J. M. Hovem, M. D. Richardson, and R. D. Stoll (eds.), Shear Waves in Marine Sediments, Kluwer Academic Publishers, Dordrecht, The Netherlands, 3-12.

Tindle, C. T., 1982. Attenuation parameters from normal mode measurements. J. Acoust. Soc. Am., 71(5), 1145-1148.

Tucholke, B. E., Macdonald, K. D., and Fox P. J., 1991. ONR seafloor Natural Laboratories on slow-and fast-spreading mid-ocean ridges. EOS, Trans. Amer. Geophys. Union, 72, 268-270.

Tyce, R. C., 1976. Near-bottom observations of 4 kHz acoustic reflectivity and attenuation. Geophysics, 41(4), 673-699.

Tyce, R. C., 1981. Estimating acoustic attenuation from a quantitative seismic profiler. Geophysics, 46(10), 1364-1378.

Ulonska, A., 1968. Versuche zur messung der schallgeschwindigkeit und schalldampfung im sediment in situ. Deut. Hydrogr. Z., Jahr. 2, Heft 2, 49-58.

Urmos, J. and Wilkens, R. H., 1993. In situ velocities in pelagic carbonates: new insights from Ocean Drilling Leg 130, Ontong Java Plateau. J. Geophys. Res., 98, 7903-7920.

Warrick, R., 1974. Seismic investigation of a San Francisco Bay mud site. Bull. Seis. Soc. Am., 64(2), 375-385.

Whitmarsh, R. B. and Miles, P. R., 1990. In situ measurements of shear-wave velocity in ocean sediments. In J. M. Hovem, M. D. Richardson, and R. D. Stoll (eds.), Shear Waves in Marine Sediments, Kluwer Academic Publishers, Dordrecht, The Netherlands, 321-328.

Winterer, et al., 1973. Initial Reports Deep Sea Drilling Project, Vol. XVII, U.S. Government Printing Office, Washington D.C., 930 p.

Wood, A. B. and Weston, D. E., 1964. The propagation of sound in mud. Acustica, 14, 156-162.

Wrolstad, K., 1980. Interval velocity and attenuation measurements in sediments from marine seismic reflection data. J. Acoust. Soc. Am., 68(5), 1415-1435.

Yeats, R. S., et al., 1981. Site 469. Initial Reports Deep Sea Drilling Project, Vol. LXIII, U.S. Government Printing Office, Washington D.C., 173-189.

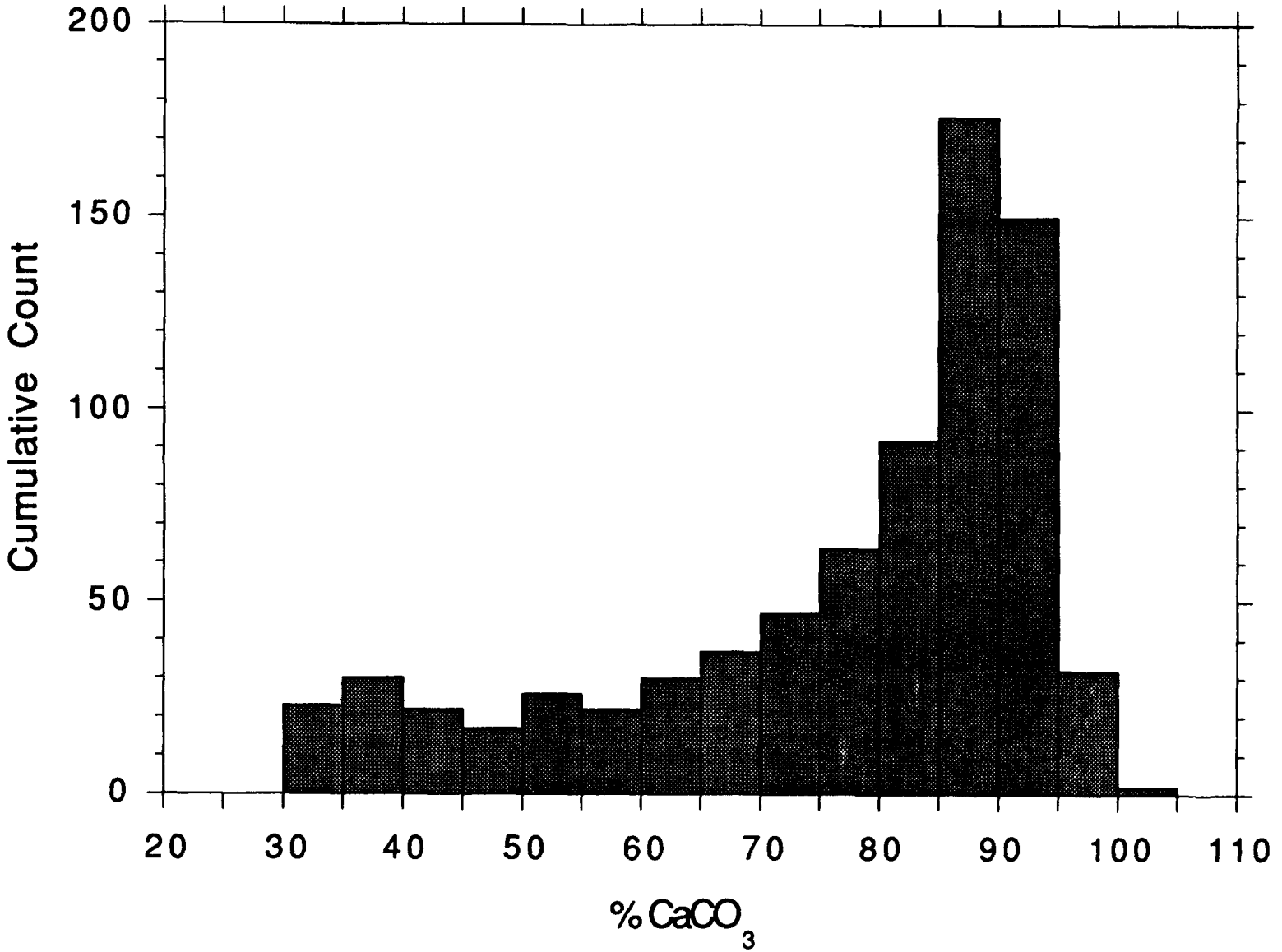
200
150
100
50
0
Cumulative Count
20
30
40
50
60
70
80
90
100
110
% CaCO3

Fig. 1

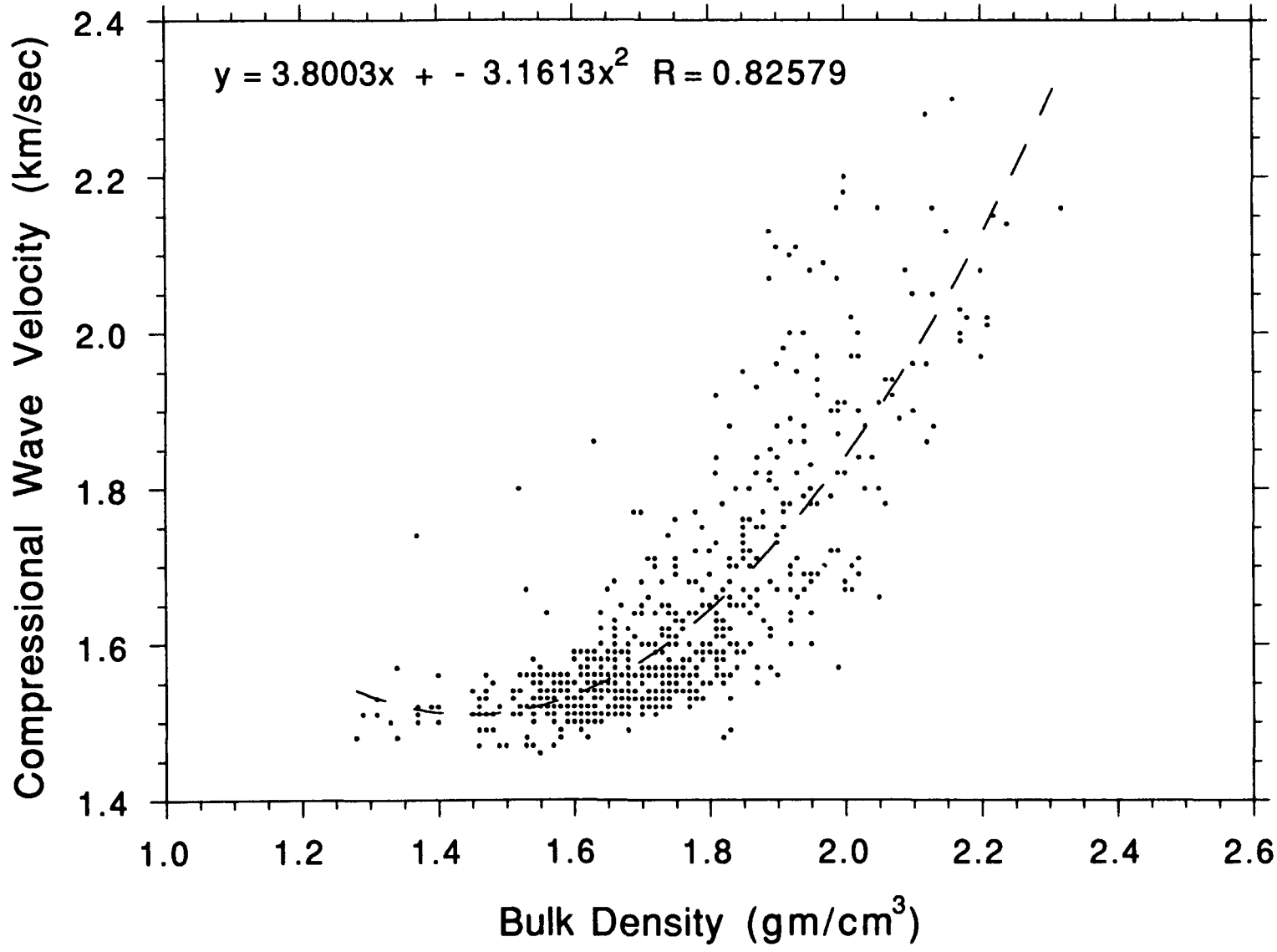
y = 3.8003x + - 3.1613x2 R = 0.82579
Compressional Wave Velocity (km/sec)
2.4
2.2
2.0
1.8
1.6
1.4
1.0
1.2
1.4
1.6
1.8
2.0
2.2
2.4
2.6
Bulk Density (gm/cm3)

Fig. 2

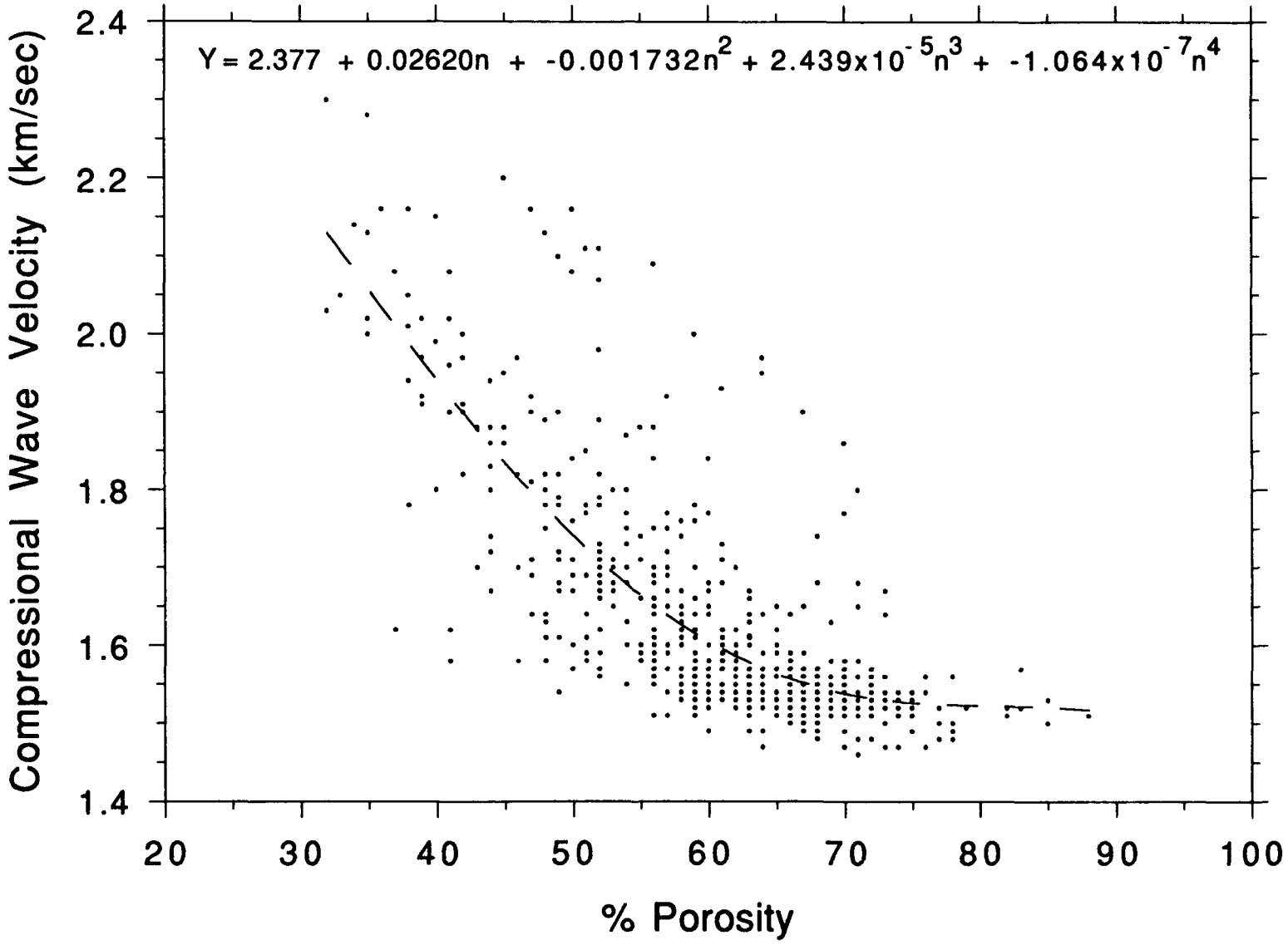
Y = 2.377 + 0.02620n + -0.001732n^2 + 2.439x10^-5 n^3 + -1.064x10^-7 n^4
Compressional Wave Velocity (km/sec)
2.4
2.2
2.0
1.8
1.6
1.4
20
30
40
50
60
70
80
90
100
% Porosity

Fig. 3

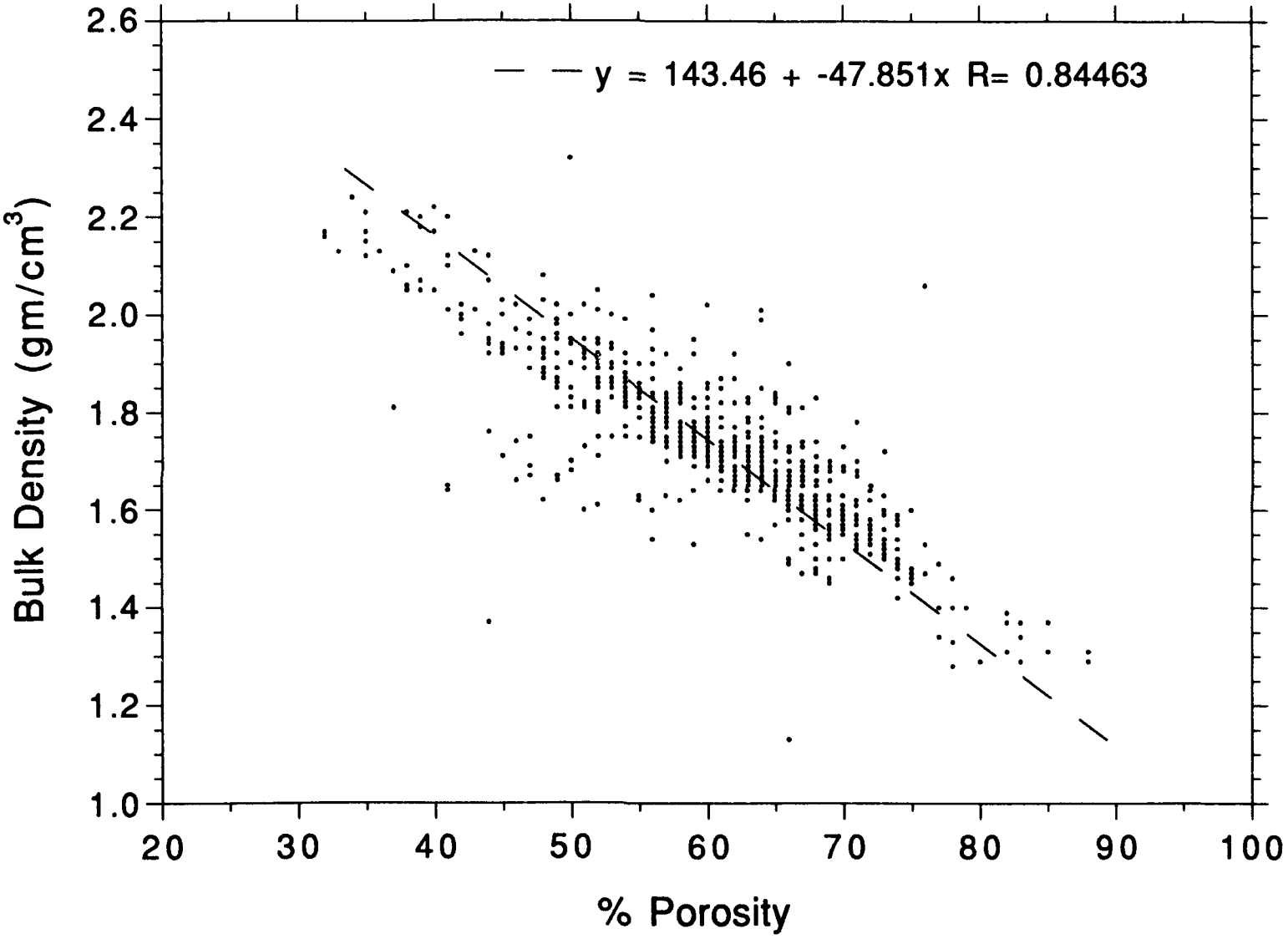
y = 143.46 + -47.851x R= 0.84463
Bulk Density (gm/cm3)
% Porosity
2.6
2.4
2.2
2.0
1.8
1.6
1.4
1.2
1.0
20
30
40
50
60
70
80
90
100

Fig. 4

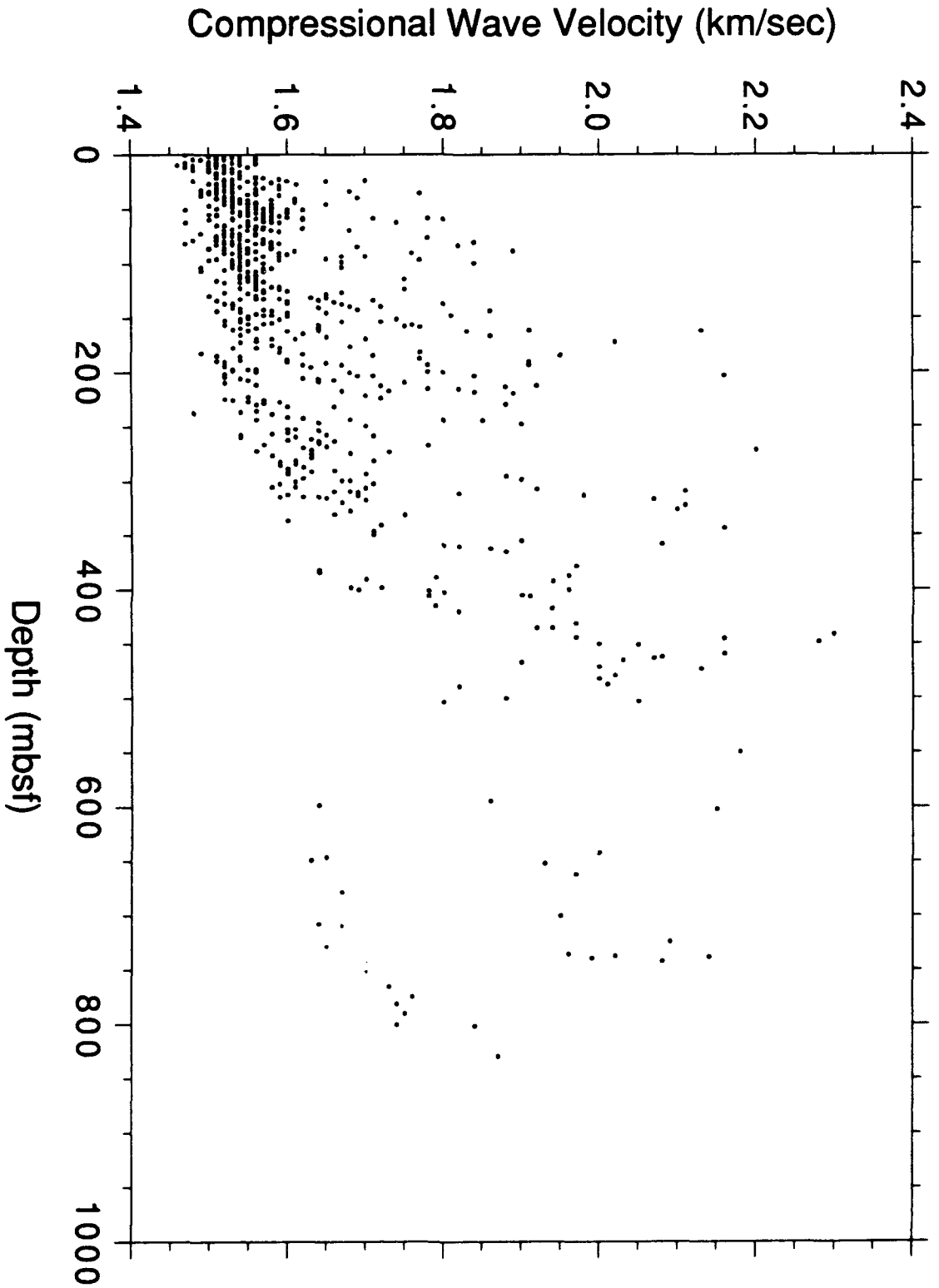
Compressional Wave Velocity (km/sec)
1.4
1.6
1.8
2.0
2.2
2.4
0
200
400
600
800
1000
Depth (mbsf)

Fig. 5

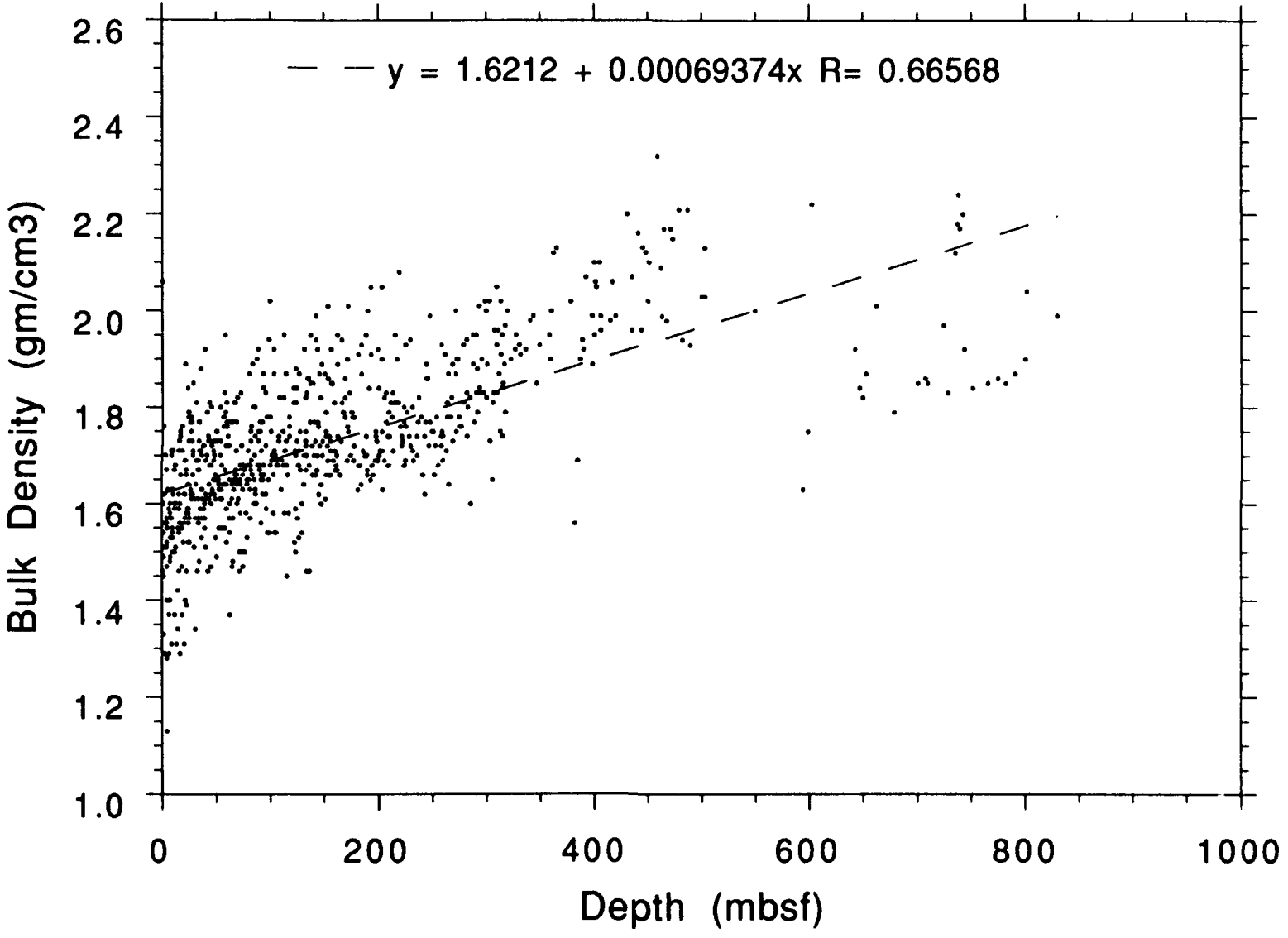
y = 1.6212 + 0.00069374x R= 0.66568
Bulk Density (gm/cm3)
2.6
2.4
2.2
2.0
1.8
1.6
1.4
1.2
1.0
0
200
400
600
800
1000
Depth (mbsf)

Fig. 6

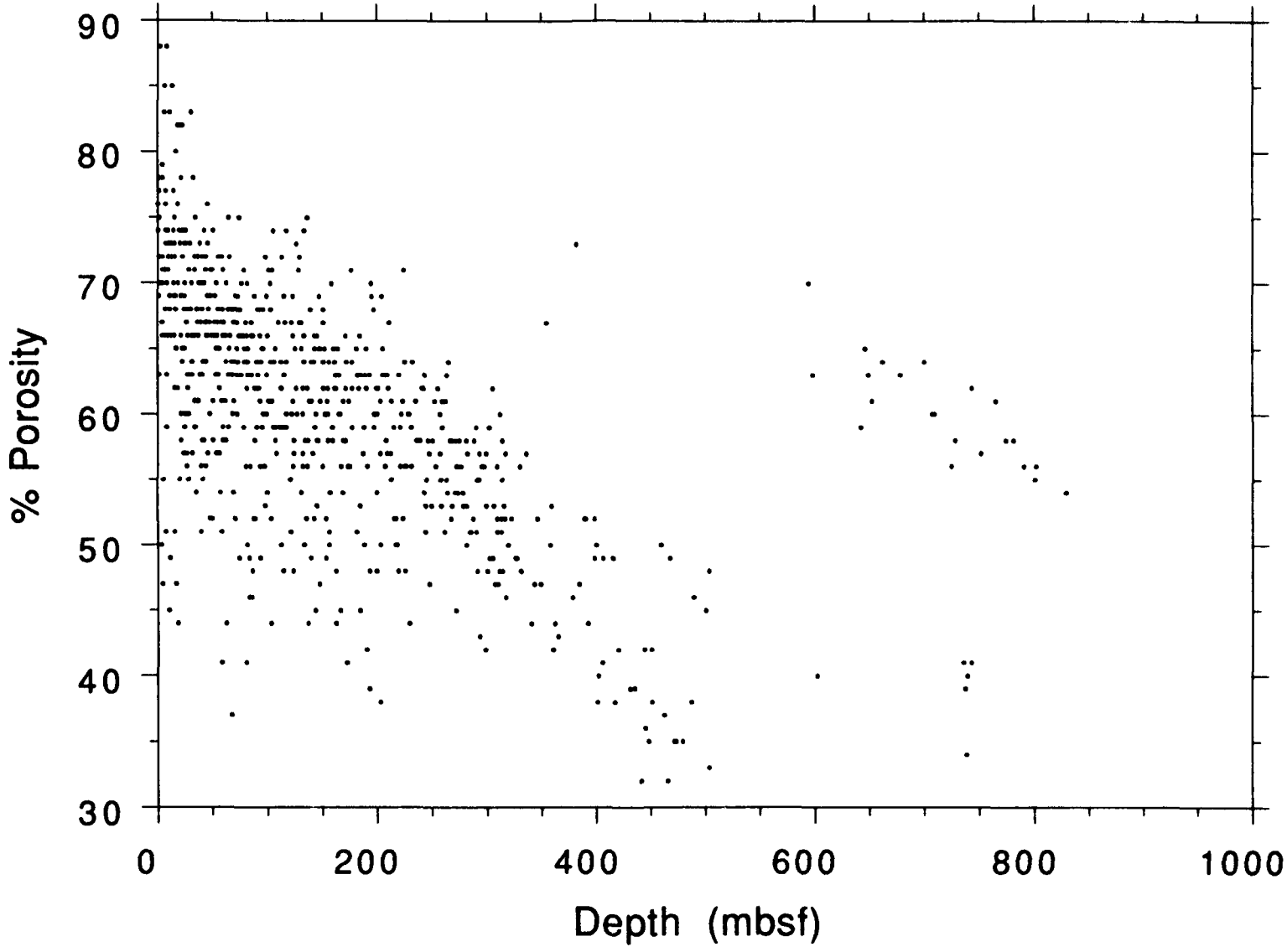

Fig. 7

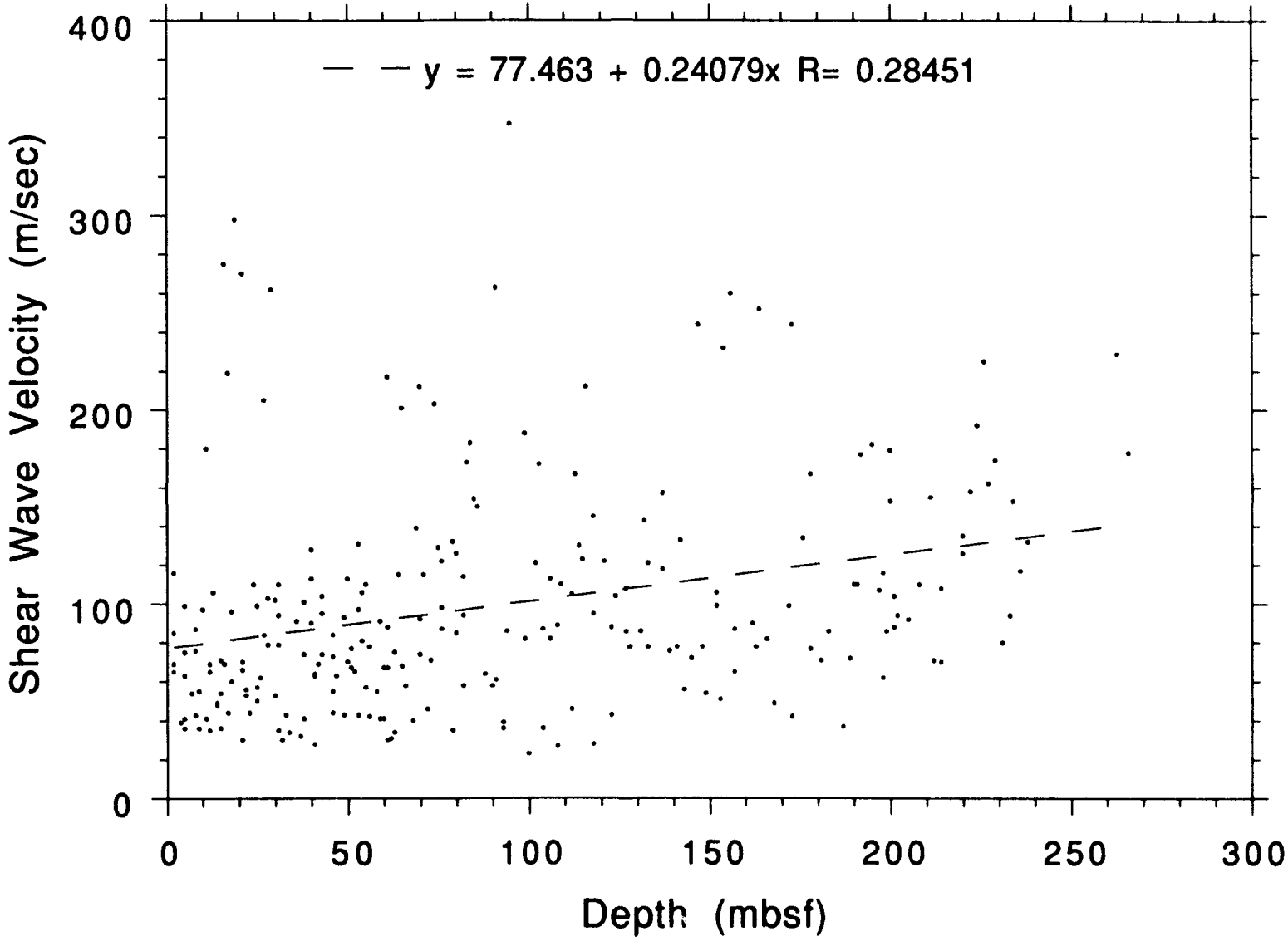
y = 77.463 + 0.24079x R= 0.28451
Shear Wave Velocity (m/sec)
400
300
200
100
0
0
50
100
150
200
250
300
Depth (mbsf)

Fig. 8

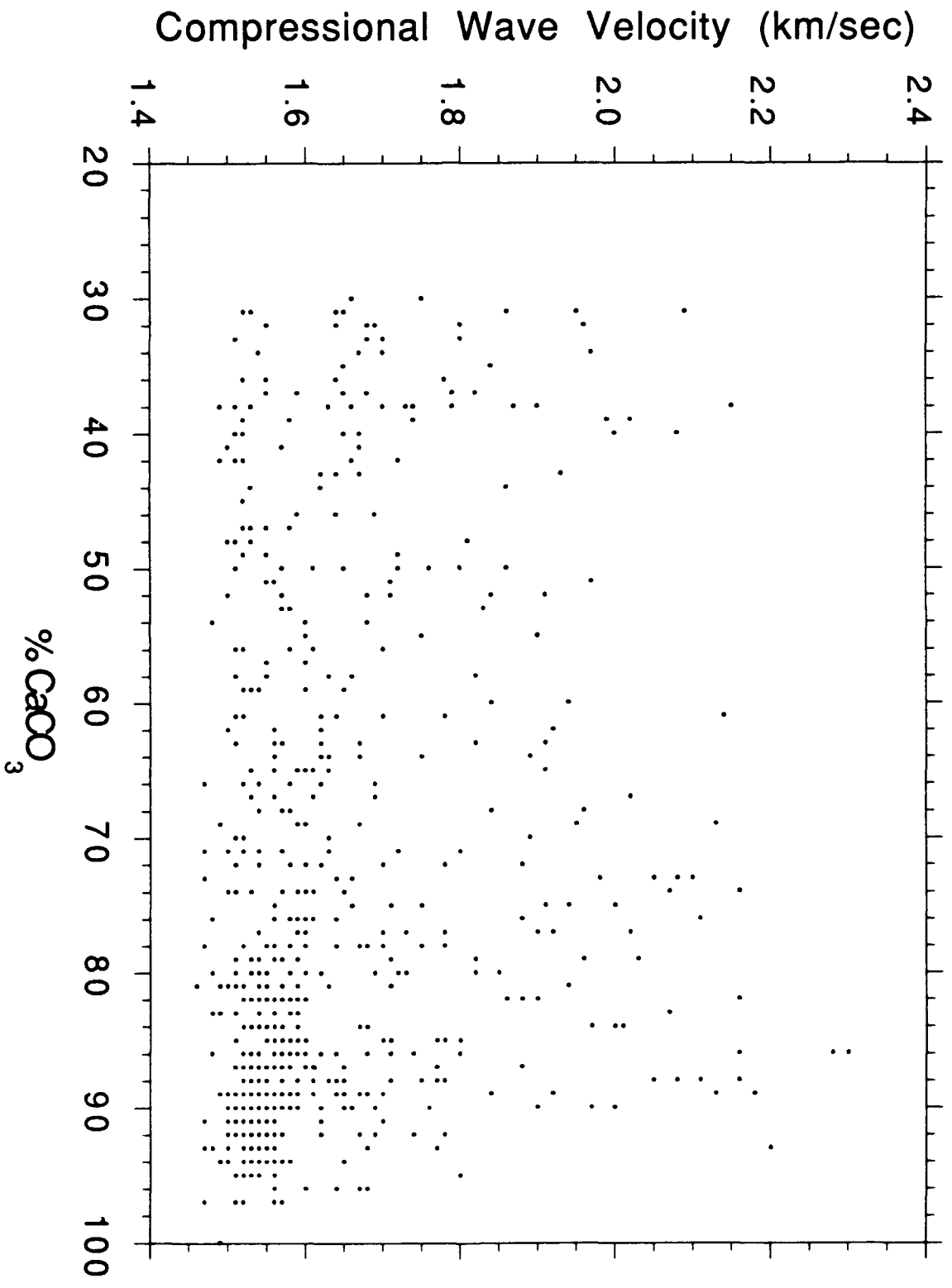
Compressional Wave Velocity (km/sec)
1.4
1.6
1.8
2.0
2.2
2.4
20
30
40
50
60
70
80
90
100
% CaCO3

Fig. 9

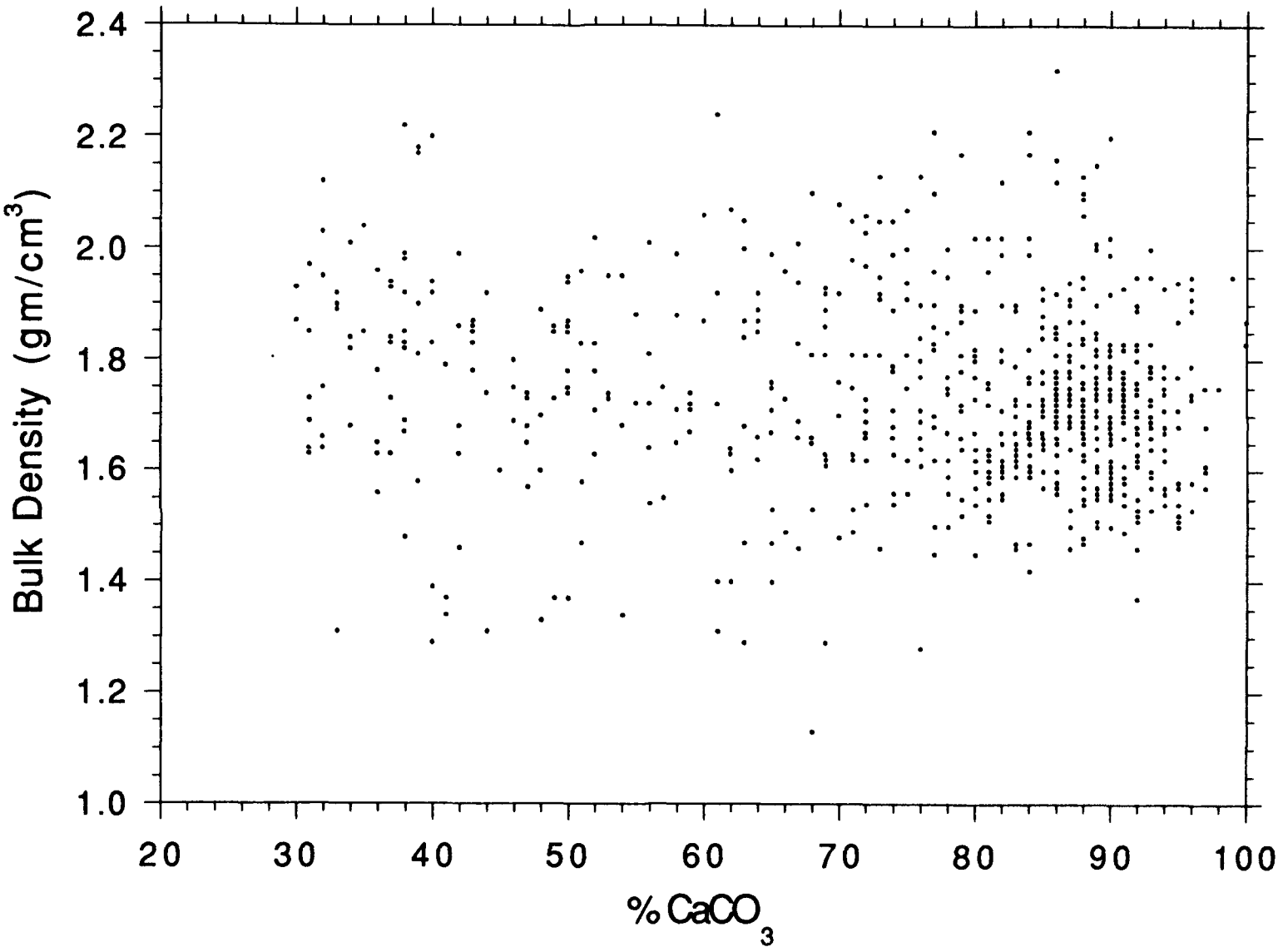
Bulk Density (gm/cm3)
2.4
2.2
2.0
1.8
1.6
1.4
1.2
1.0
20
30
40
50
60
70
80
90
100
% CaCO3

Fig. 10

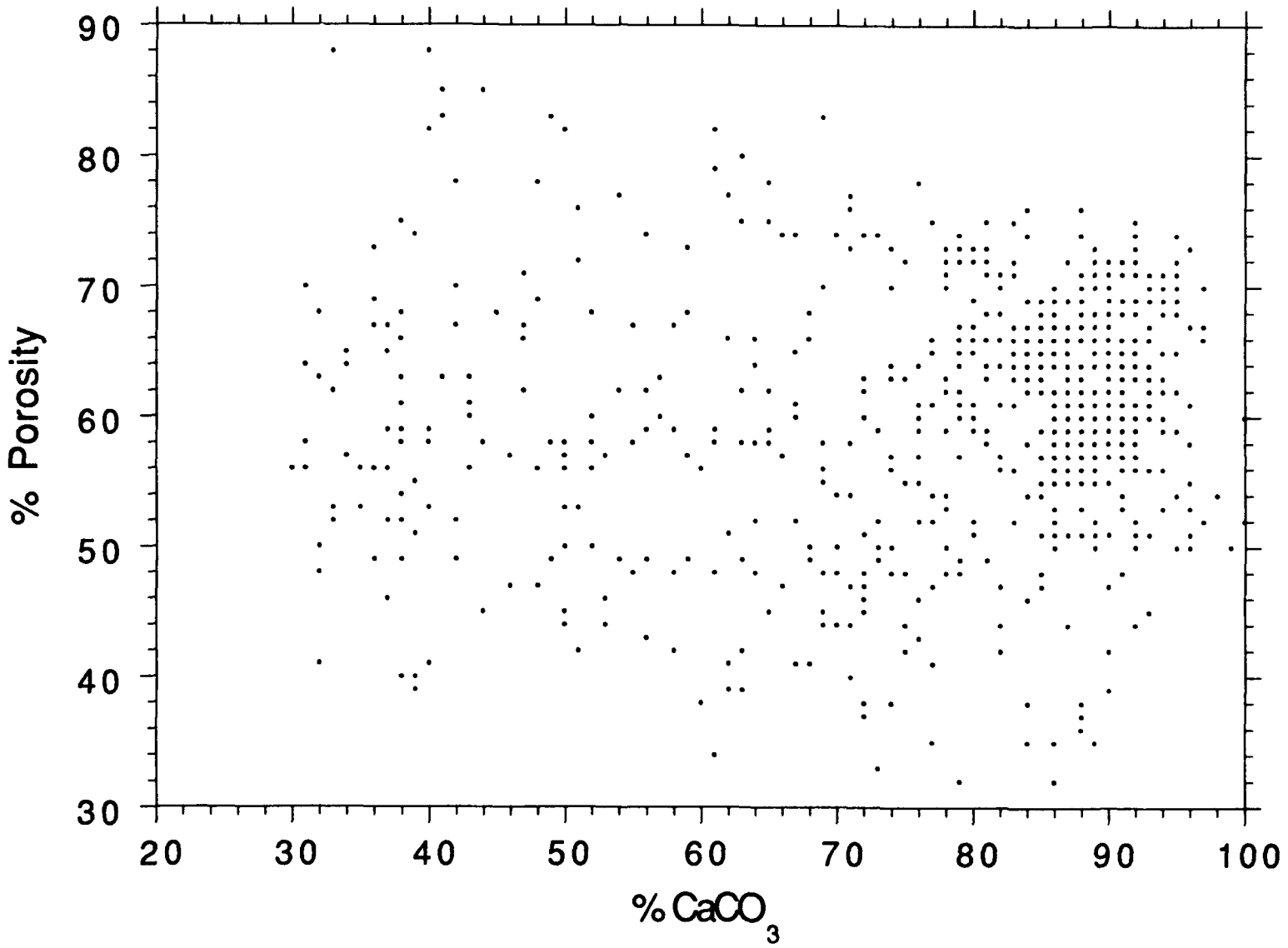

Fig. 11

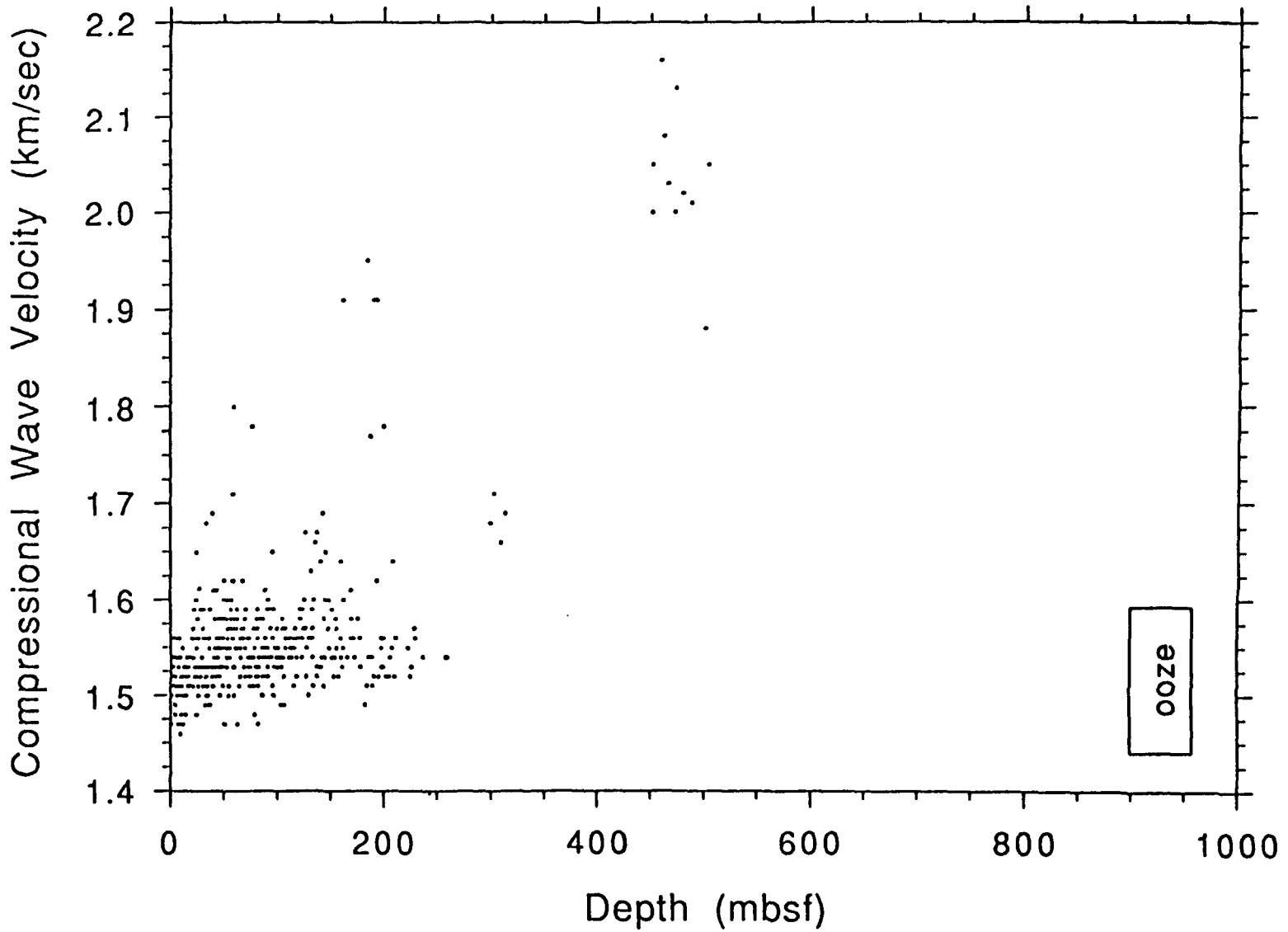
Compressional Wave Velocity (km/sec)
2.2
2.1
2.0
1.9
1.8
1.7
1.6
1.5
1.4
0
200
400
600
800
1000
Depth (mbsf)
ooze

Fig. 12

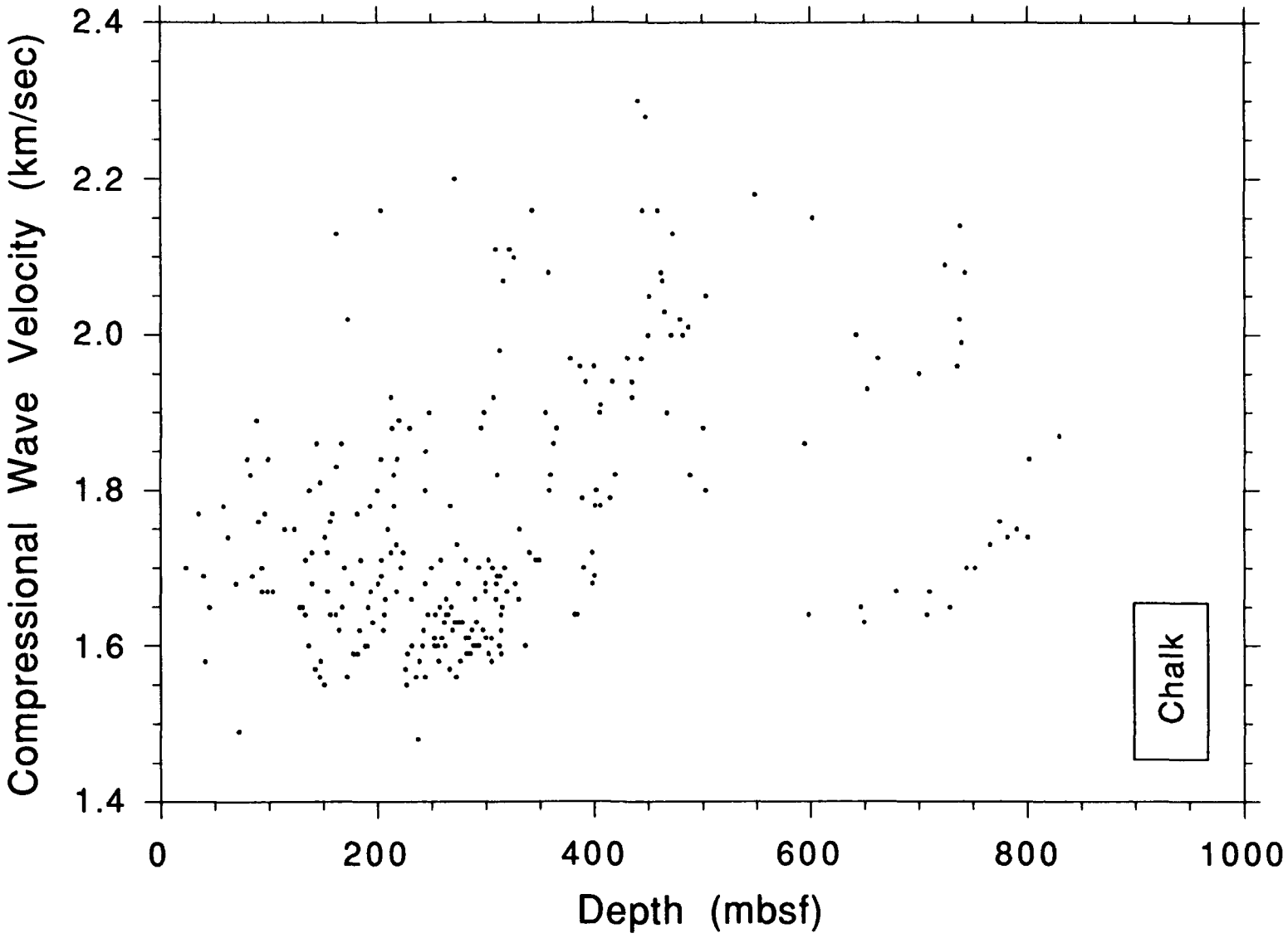
Compressional Wave Velocity (km/sec)
2.4
2.2
2.0
1.8
1.6
1.4
0
200
400
600
800
1000
Depth (mbsf)
Chalk

Fig. 13

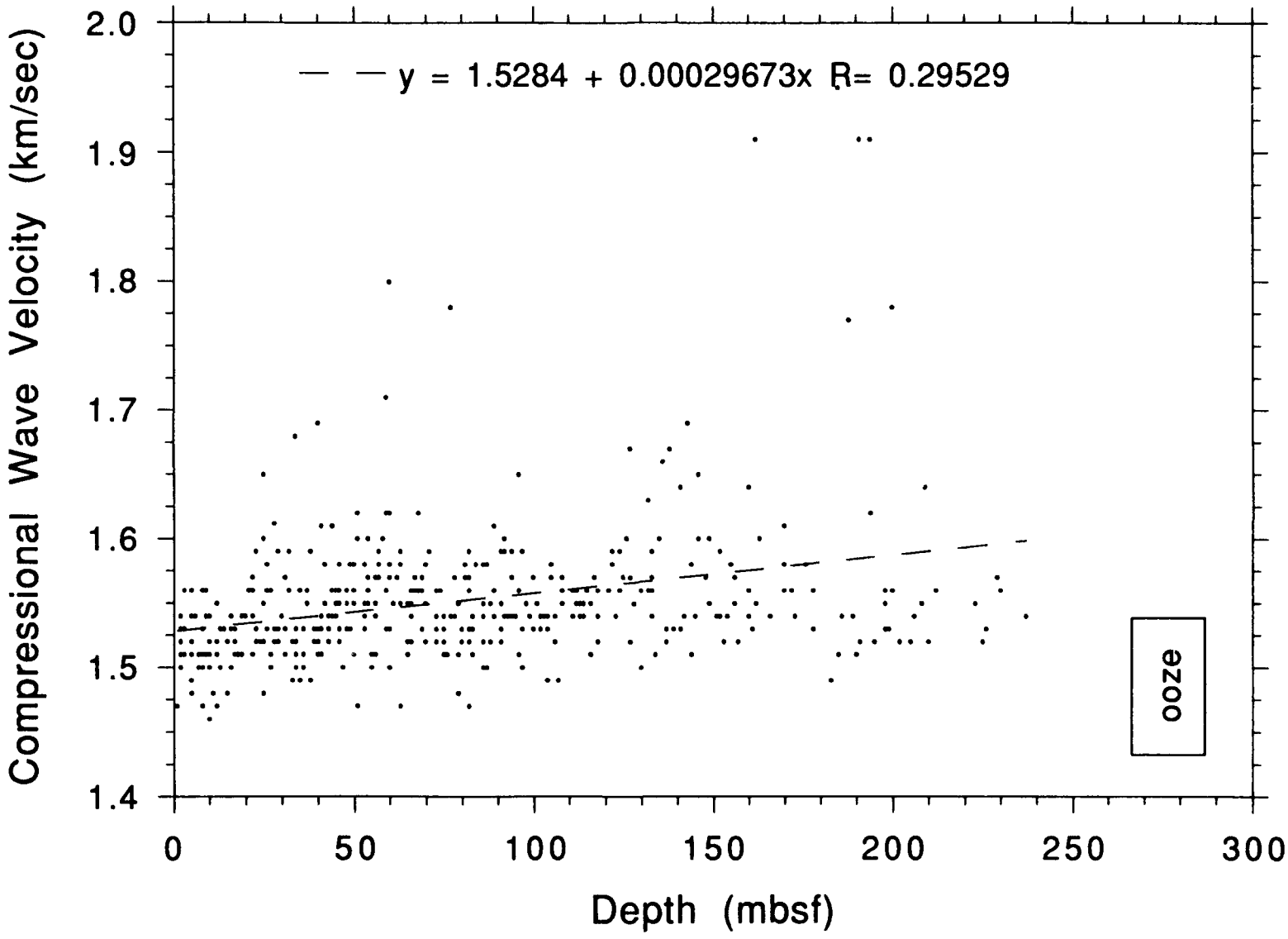
y = 1.5284 + 0.00029673x R= 0.29529
Compressional Wave Velocity (km/sec)
2.0
1.9
1.8
1.7
1.6
1.5
1.4
0
50
100
150
200
250
300
Depth (mbsf)
ooze

Fig. 14

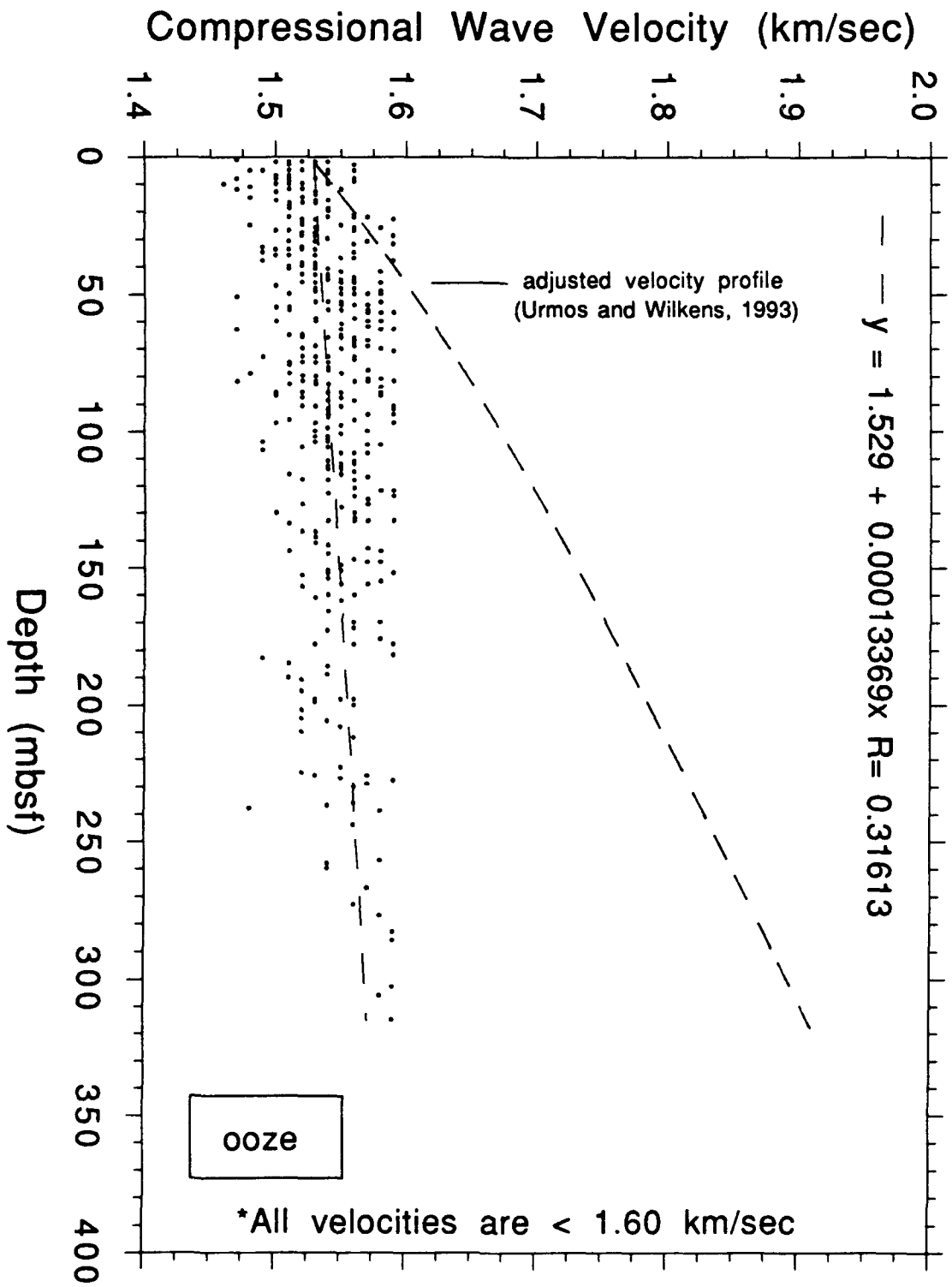
Compressional Wave Velocity (km/sec)
1.4
1.5
1.6
1.7
1.8
1.9
2.0
Depth (mbsf)
0
50
100
150
200
250
300
350
400
adjusted velocity profile
(Urmos and Wilkens, 1993)
y = 1.529 + 0.00013369x R= 0.31613
ooze
*All velocities are < 1.60 km/sec

Fig. 15

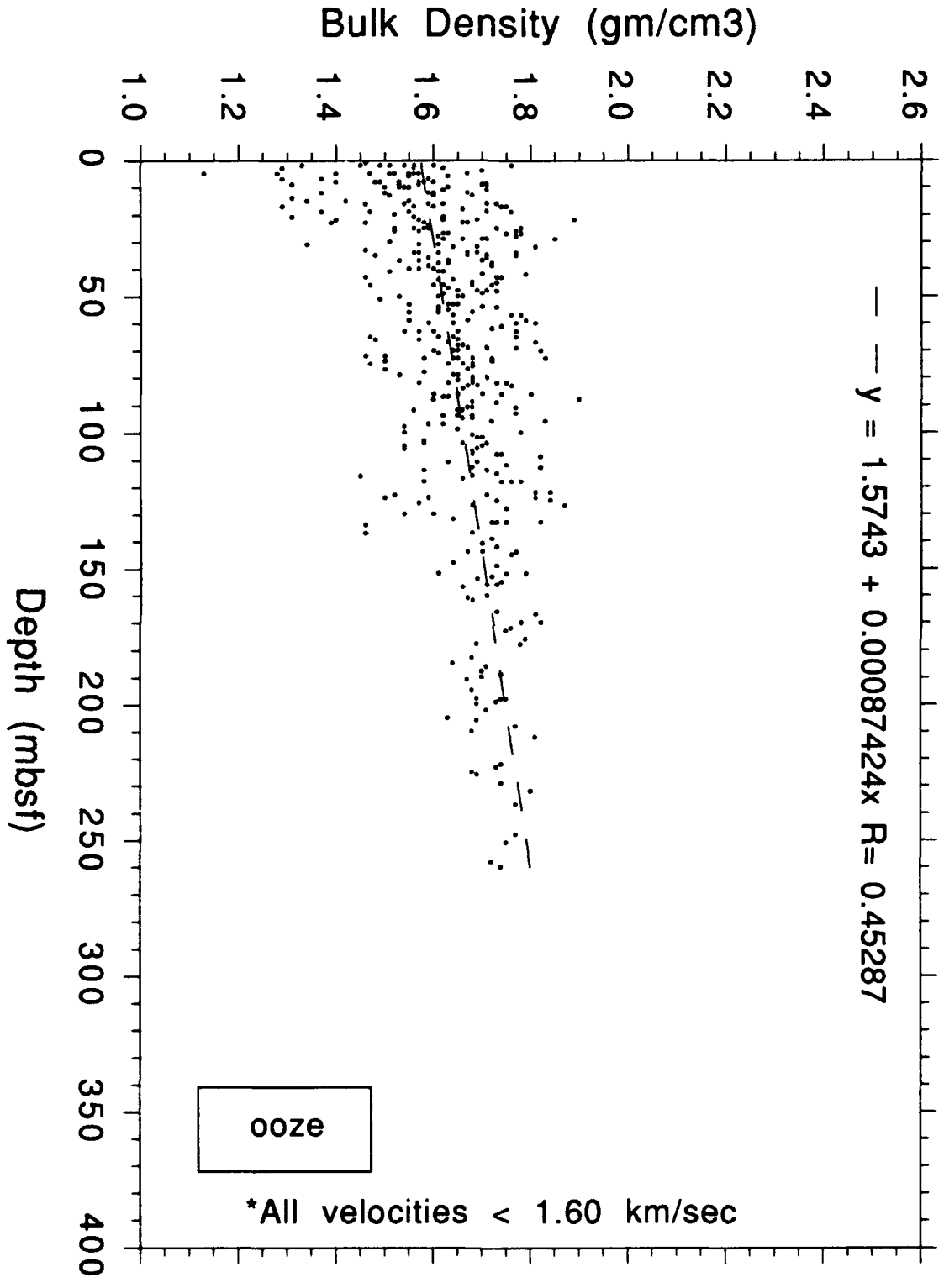
Bulk Density (gm/cm3)
1.0
1.2
1.4
1.6
1.8
2.0
2.2
2.4
2.6
Depth (mbsf)
0
50
100
150
200
250
300
350
400
y = 1.5743 + 0.00087424x R= 0.45287
ooze
*All velocities < 1.60 km/sec

Fig. 16

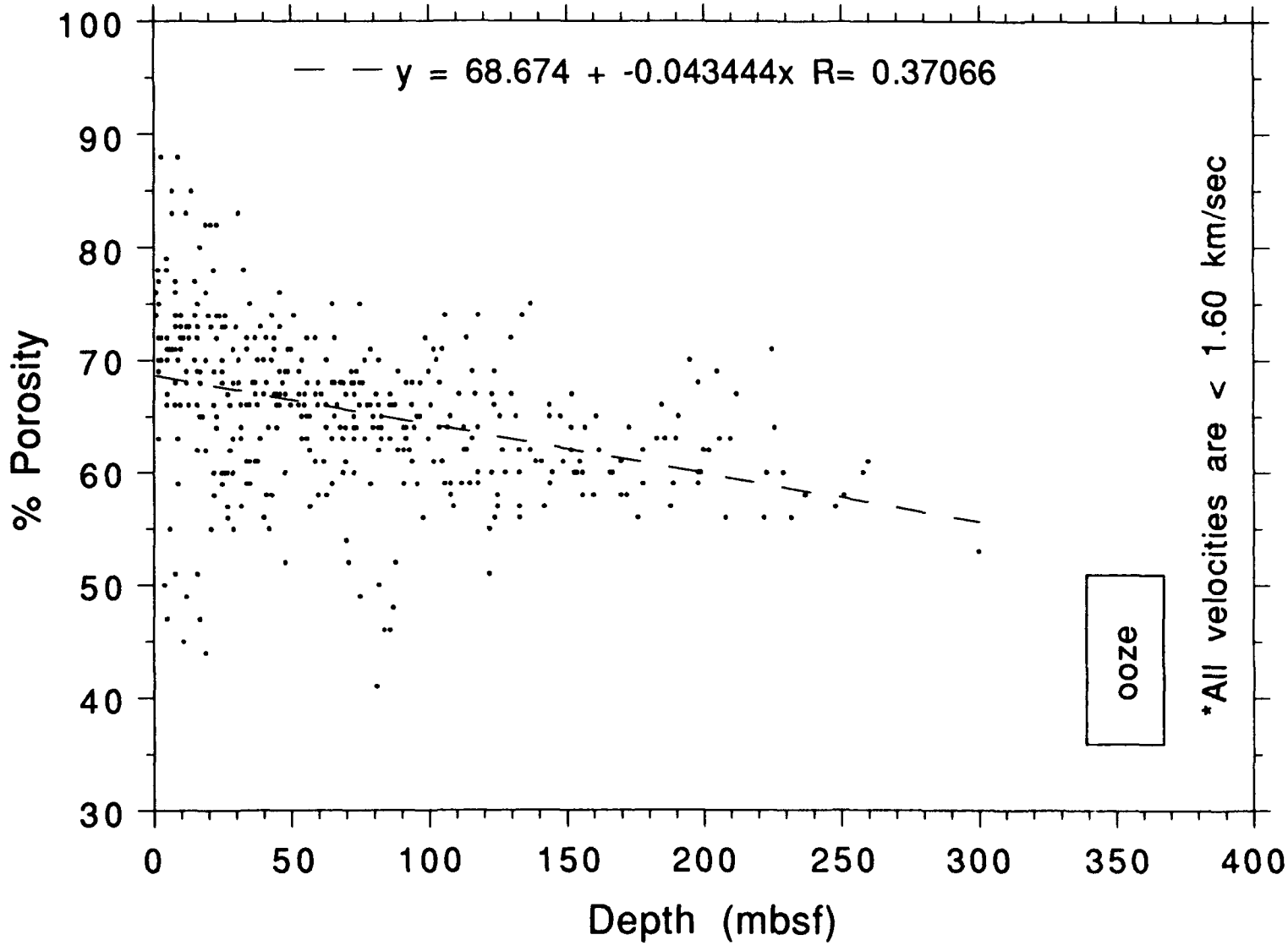
y = 68.674 + -0.043444x R= 0.37066
% Porosity
Depth (mbsf)
100
90
80
70
60
50
40
30
0
50
100
150
200
250
300
350
400
ooze
*All velocities are < 1.60 km/sec

Fig. 17

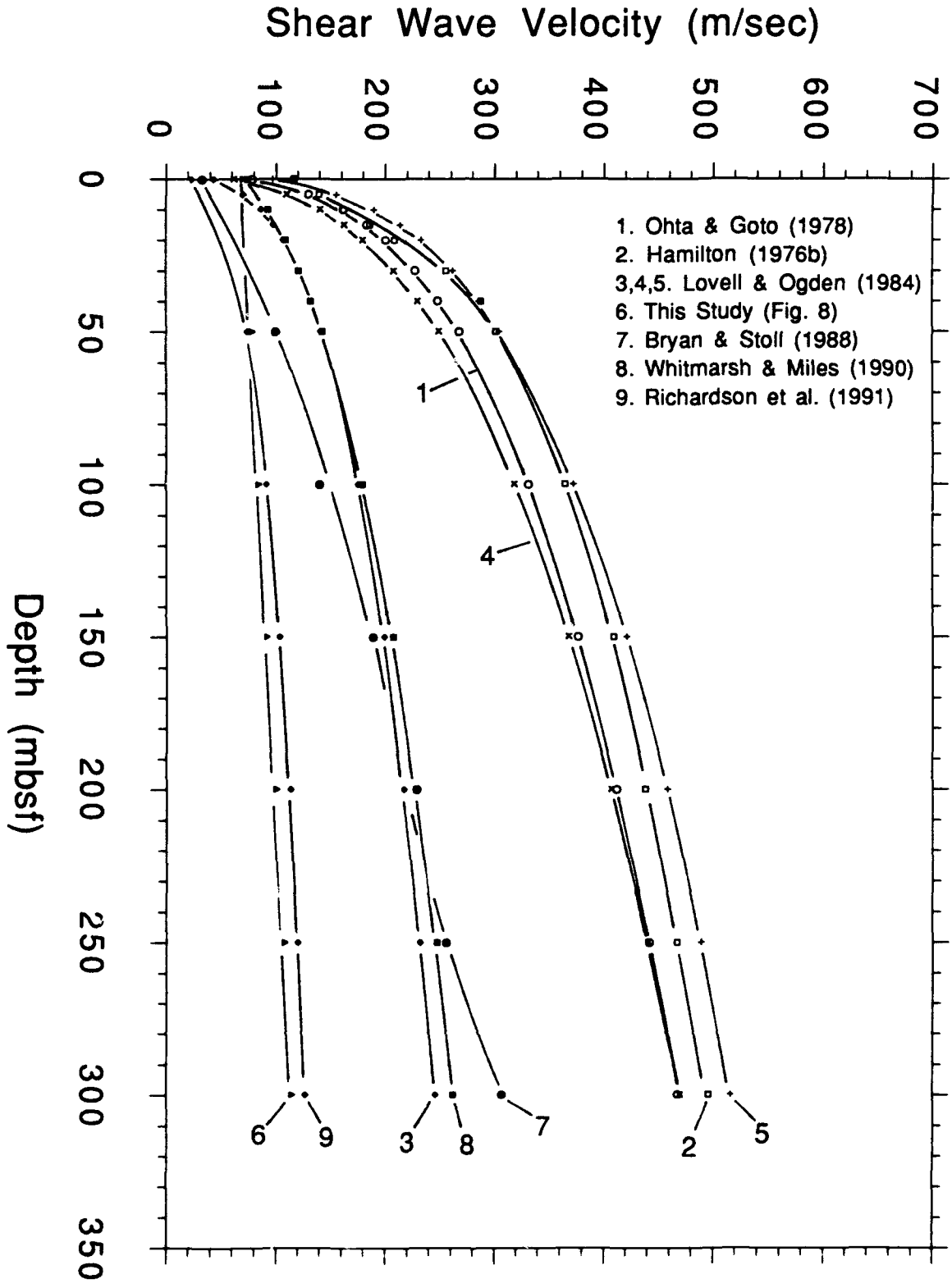
Shear Wave Velocity (m/sec)
0
100
200
300
400
500
600
700
Depth (mbsf)
0
50
100
150
200
250
300
350
1. Ohta & Goto (1978)
2. Hamilton (1976b)
3,4,5. Lovell & Ogden (1984)
6. This Study (Fig. 8)
7. Bryan & Stoll (1988)
8. Whitmarsh & Miles (1990)
9. Richardson et al. (1991)
1
4
6
9
3
8
7
2
5

Fig. 18

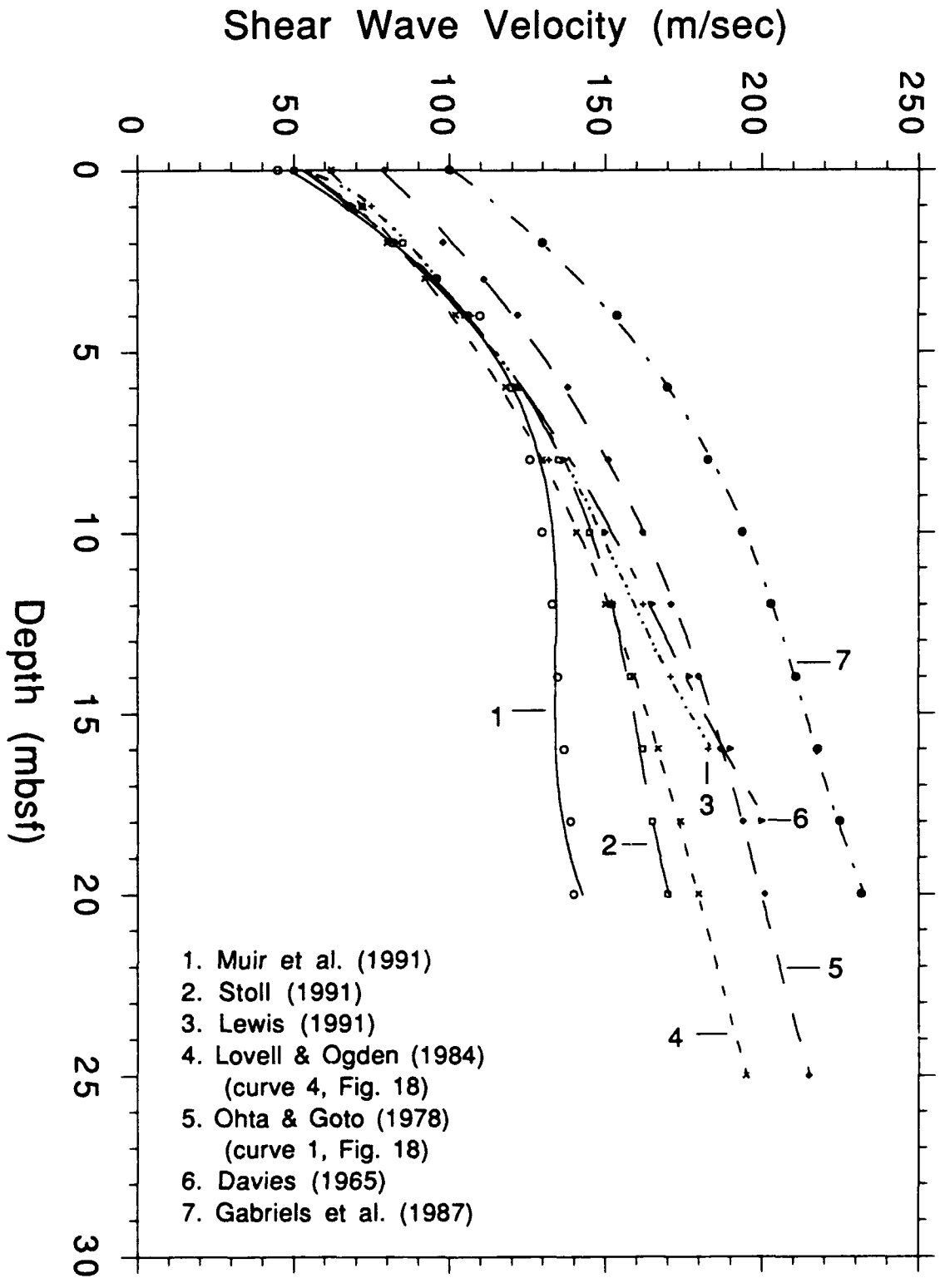
Shear Wave Velocity (m/sec)
0
50
100
150
200
250
Depth (mbsf)
0
5
10
15
20
25
30
1
2
3
4
5
6
7
1. Muir et al. (1991)
2. Stoll (1991)
3. Lewis (1991)
4. Lovell & Ogden (1984)
(curve 4, Fig. 18)
5. Ohta & Goto (1978)
(curve 1, Fig. 18)
6. Davies (1965)
7. Gabriels et al. (1987)

Fig. 19

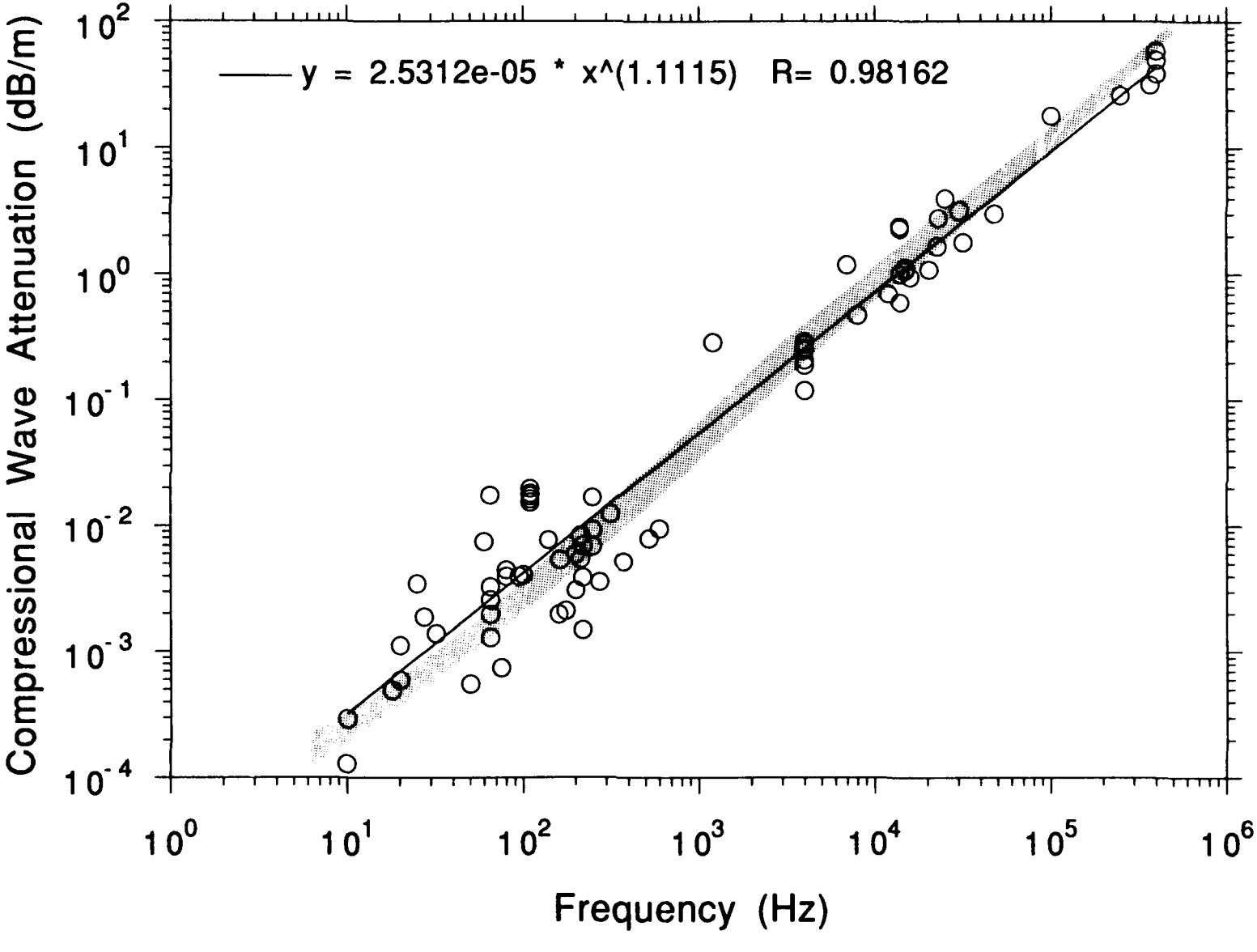
y = 2.5312e-05 * x^(1.1115) R= 0.98162
Compressional Wave Attenuation (dB/m)
Frequency (Hz)
10^2
10^1
10^0
10^-1
10^-2
10^-3
10^-4
10^0
10^1
10^2
10^3
10^4
10^5
10^6

Fig. 20

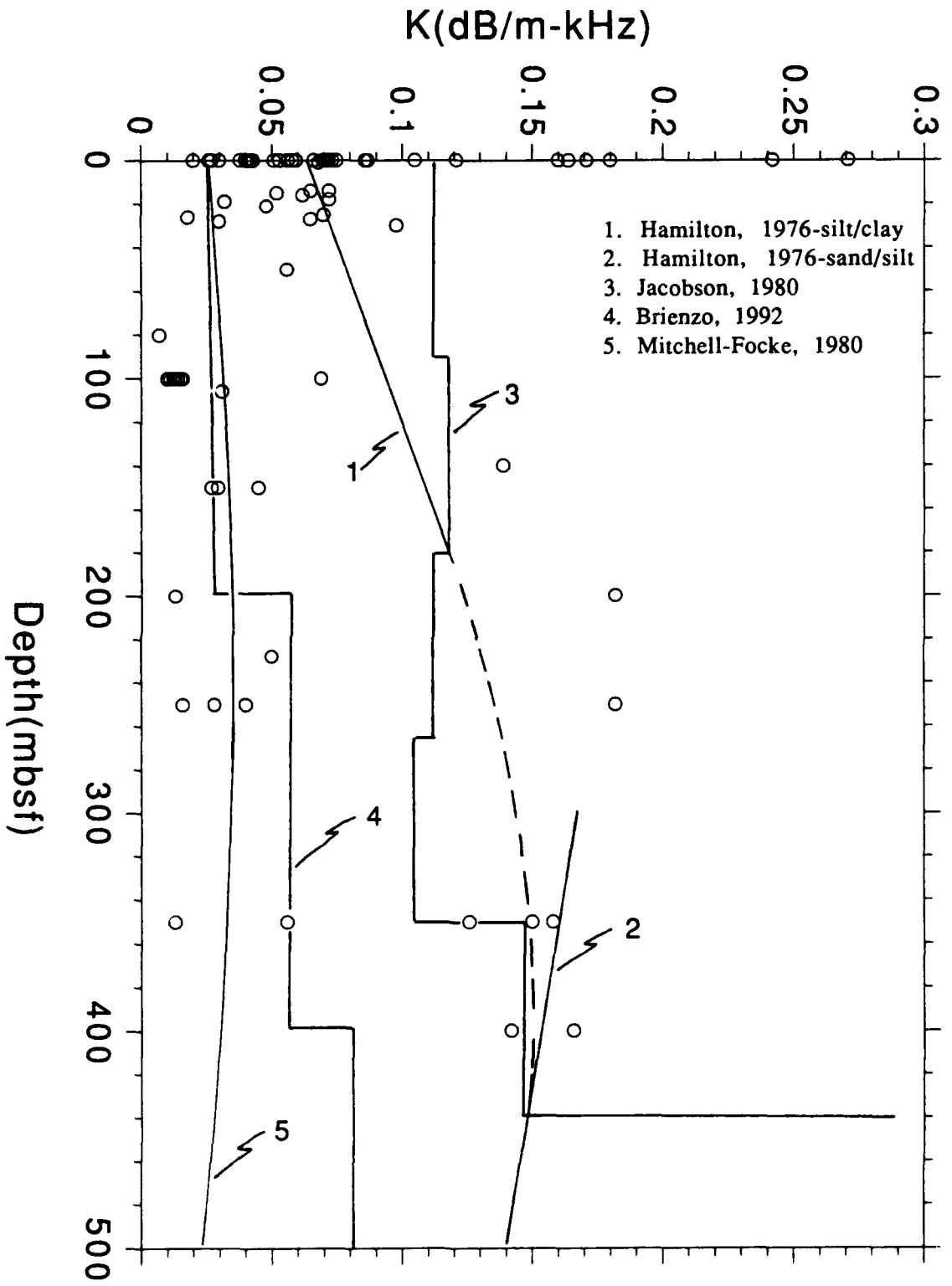
K(dB/m-kHz)
0
0.05
0.1
0.15
0.2
0.25
0.3
Depth(mbsf)
0
100
200
300
400
500
1. Hamilton, 1976-silt/clay
2. Hamilton, 1976-sand/silt
3. Jacobson, 1980
4. Brienzo, 1992
5. Mitchell-Focke, 1980
1
2
3
4
5

Fig. 21

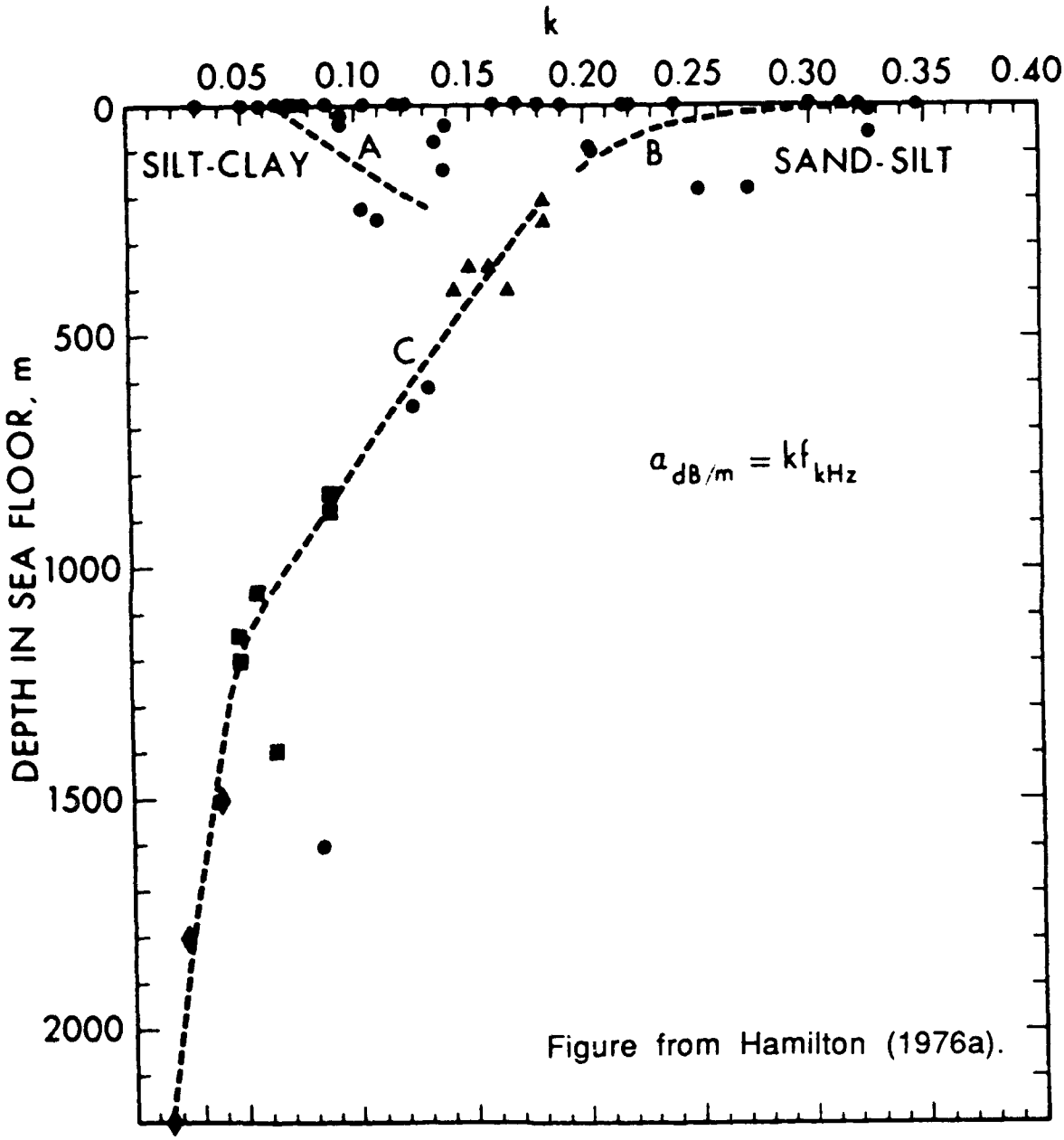
k
0.05
0.10
0.15
0.20
0.25
0.30
0.35
0.40
0
500
1000
1500
2000
DEPTH IN SEA FLOOR, m
SILT-CLAY
A
B
SAND-SILT
C
$\alpha_{dB/m} = kf_{kHz}$
Figure from Hamilton (1976a).

Fig. 22

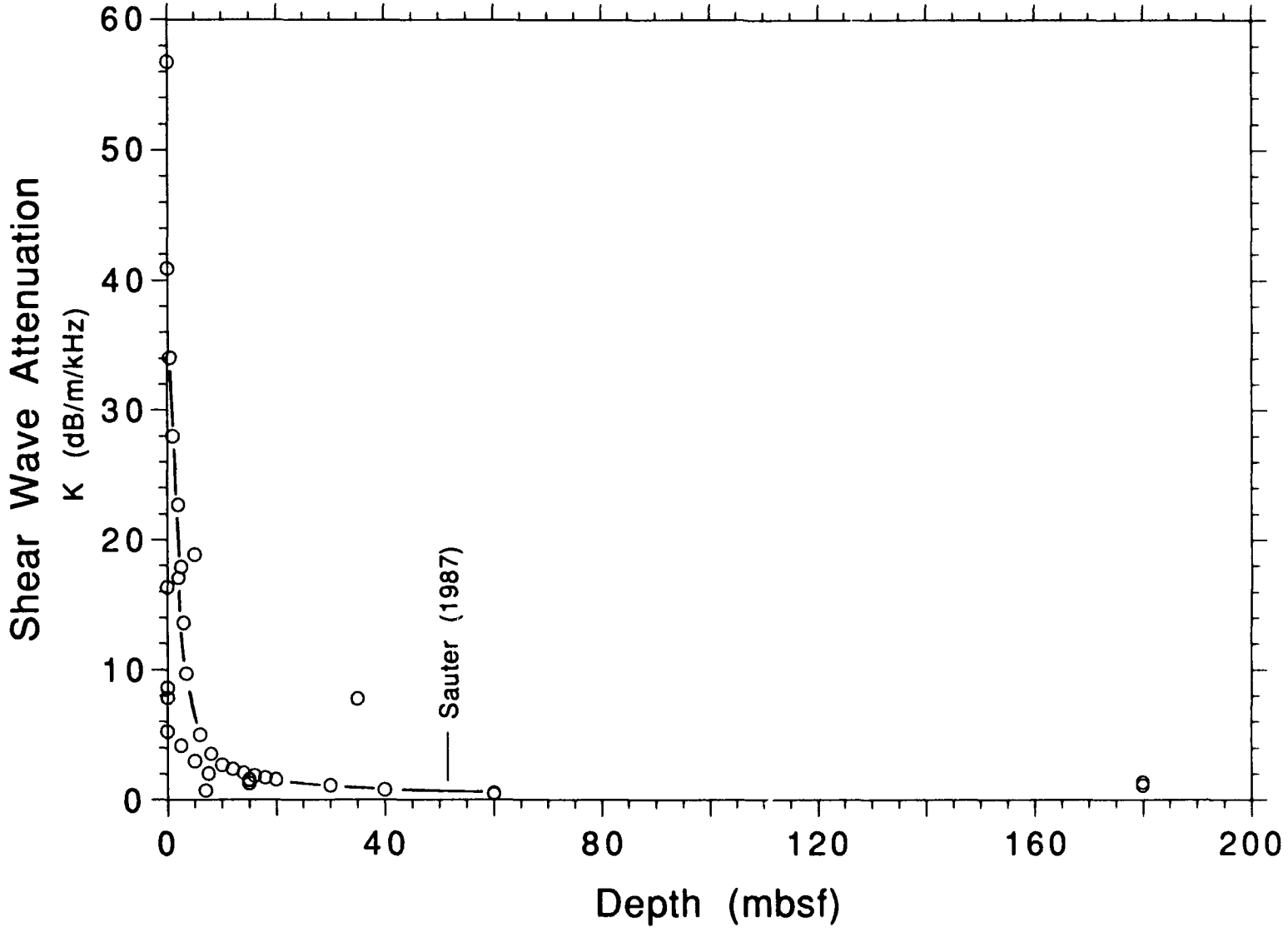
Shear Wave Attenuation
K (dB/m/kHz)
60
50
40
30
20
10
0
0
40
80
120
160
200
Depth (mbsf)
Sauter (1987)

Fig. 23

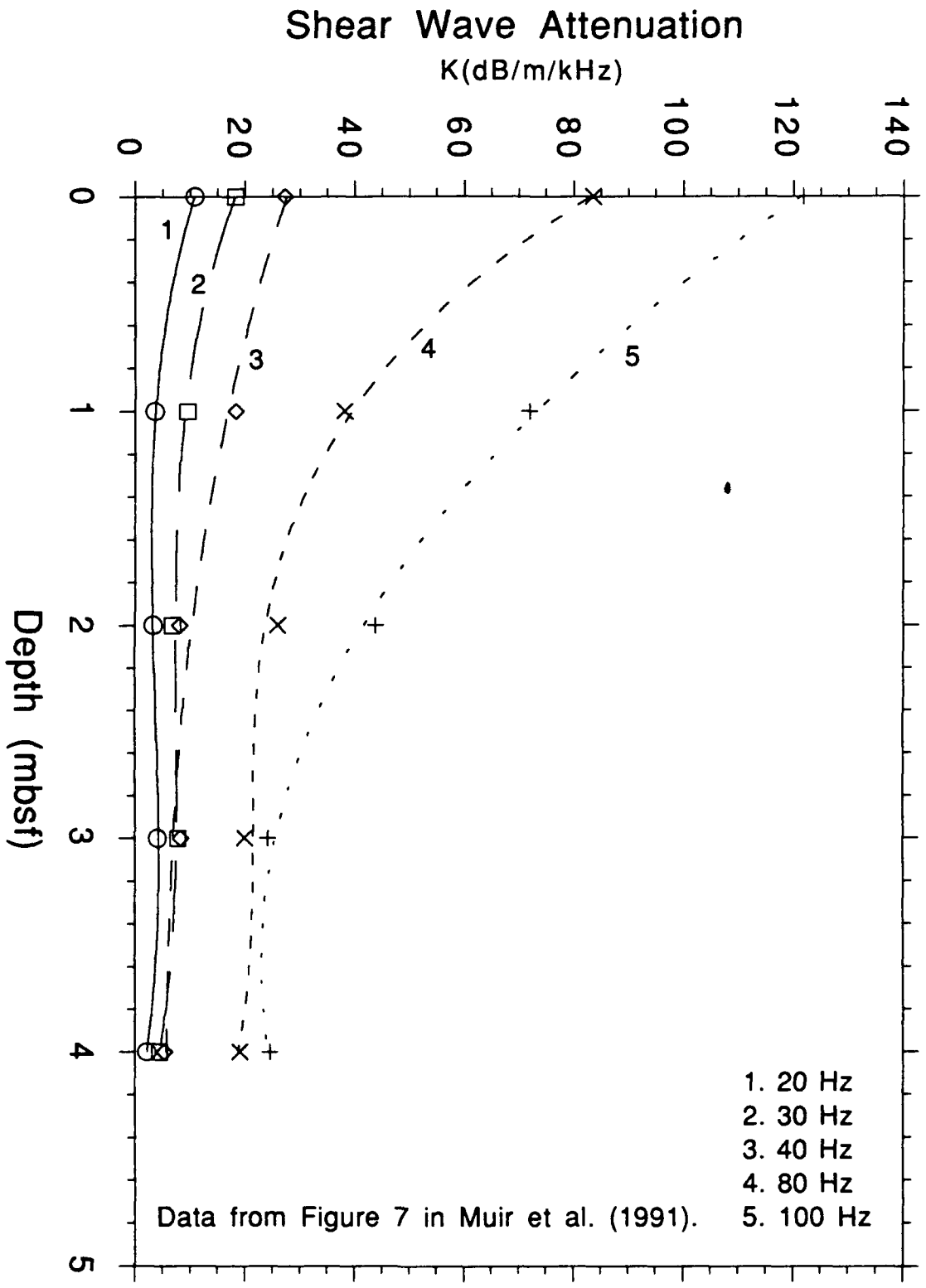
Shear Wave Attenuation
K(dB/m/kHz)
0
20
40
60
80
100
120
140
Depth (mbsf)
0
1
2
3
4
5
1
2
3
4
5
1. 20 Hz
2. 30 Hz
3. 40 Hz
4. 80 Hz
5. 100 Hz
Data from Figure 7 in Muir et al. (1991).

Fig. 24

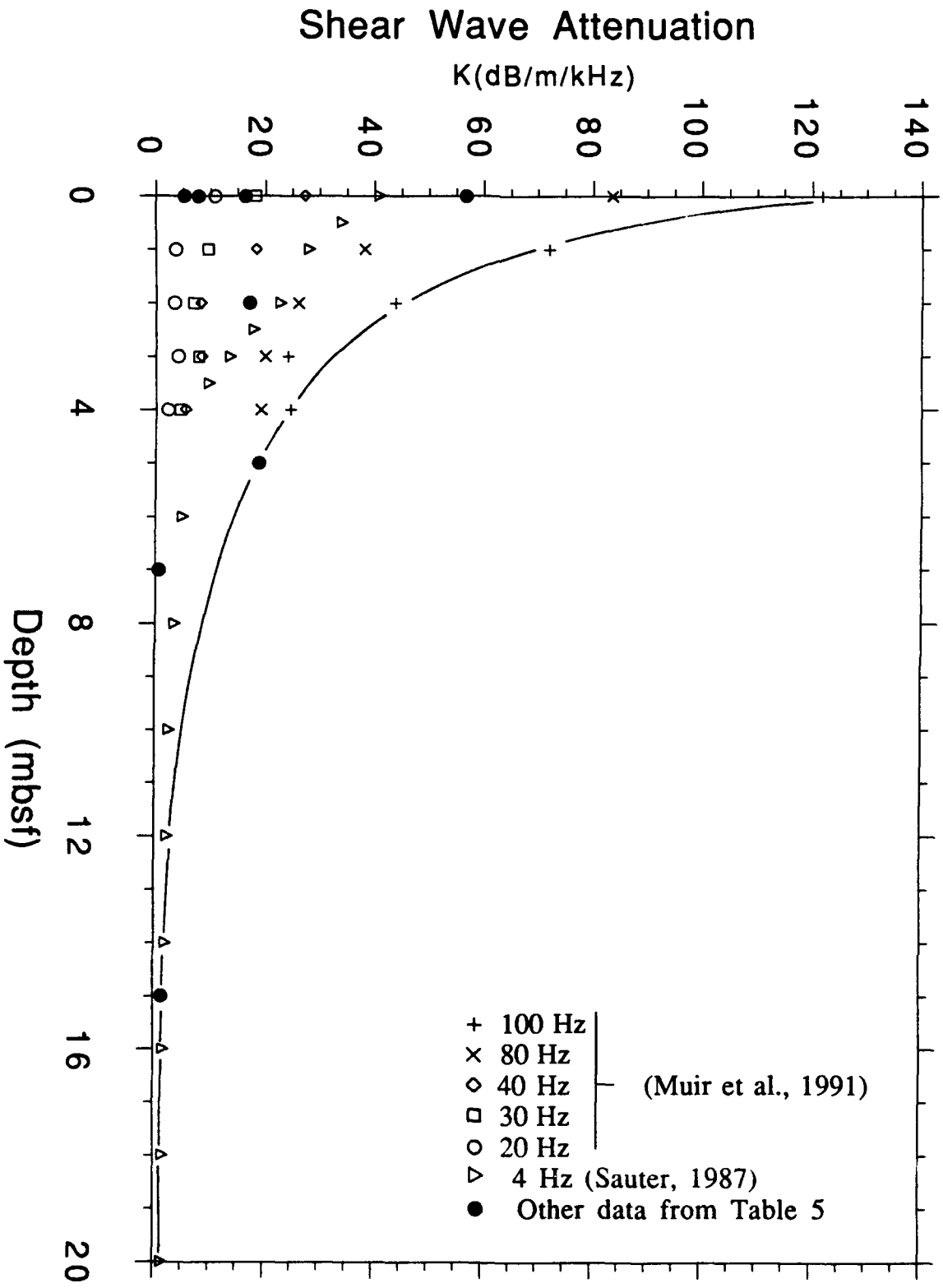
Shear Wave Attenuation
K(dB/m/kHz)
0
20
40
60
80
100
120
140
Depth (mbsf)
0
4
8
12
16
20
+ 100 Hz
× 80 Hz
◇ 40 Hz
□ 30 Hz
○ 20 Hz
(Muir et al., 1991)
▷ 4 Hz (Sauter, 1987)
● Other data from Table 5

Fig. 25

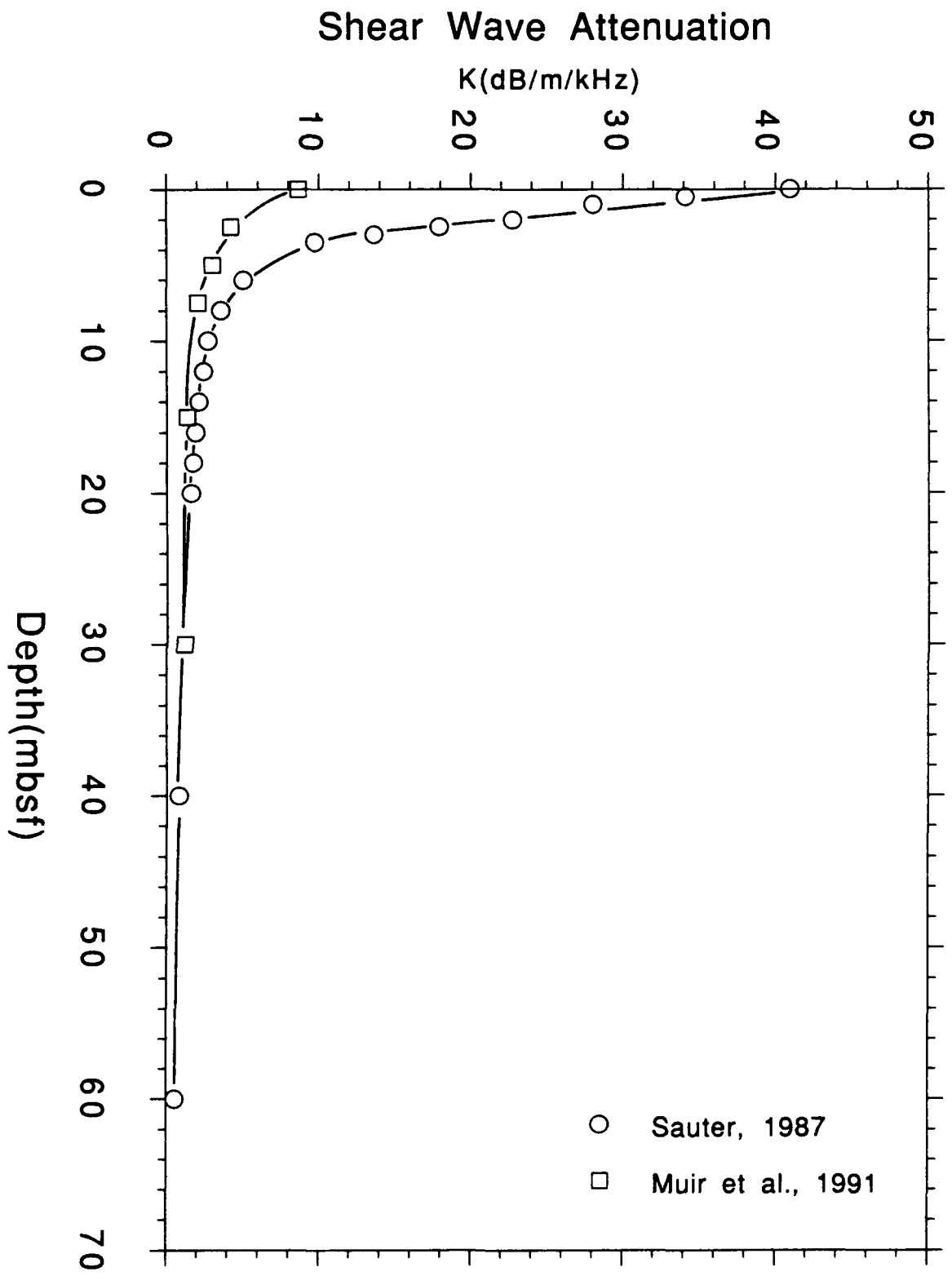
Shear Wave Attenuation
K(dB/m/kHz)
0
10
20
30
40
50
Depth(mbsf)
0
10
20
30
40
50
60
70
Sauter, 1987
Muir et al., 1991

Fig. 26